Oxidation of methyl and ethyl butanoates

Mohammed Hichem Hakka, Hayet Bennadji, Joffrey Biet, Mohammed Yahyaoui, Baptiste Sirjean, Valérie Warth, Lucie Coniglio, Olivier Herbinet, Pierre-Alexandre Glaude, Francis Billaud, et al.

Oxidation of methyl and ethyl butanoates

M. H. Hakka, H. Bennadji, J. Biet, M. Yahyaoui, B. Sirjean, V. Warth, L. Coniglio, O. Herbinet, P. A. Glaude, F. Billaud, F. Battin-Leclerc*

Université de Lorraine, CNRS, Laboratoire Réactions et Génie Procédés, 1 Rue Grandville, F-54000 Nancy, France

Abstract

This paper describes an experimental and modeling study of the oxidation of methyl and ethyl butanoates in a shock tube. The ignition delays of these two esters mixed with oxygen and argon for equivalence ratios from 0.25 to 2 and ester concentrations of 0.5% and 1% were measured behind a reflected shock wave for temperatures from 1250 to 2000 K and pressures around 8 atm. To extend the range of studied temperatures in the case of methyl butanoate, two sets of measurements were also made in a jet-stirred reactor at 800 and 850 K, at atmospheric pressure, at residence times varying between 1.5 and 9 s and for equivalence ratios of 0.5 and 1. Detailed mechanisms for the combustion of methyl and ethyl butanoates have been automatically generated using a version of EXGAS software improved to take into account these oxygenated reactants. These mechanisms have been validated through comparison of simulated and experimental results in both types of reactor. The main reaction pathways have been derived from reaction flux and sensitivity analyses performed at different temperatures.

Keywords: Benzene; Toluene; Decane; Low-temperature oxidation; Jet-stirred reactor

* Frédérique Battin-Leclerc,
Ecole Nationale Supérieure des Industries Chimiques
BP 20451
1 Rue Grandville
F-54000 Nancy
France

Introduction

Environmental concerns have led to an increased interest in the use of fuels containing a larger fraction of components that have been derived from biomass, such as methyl or ethyl esters in biodiesel (1,2). Biodiesel is composed of monoalkyl esters (methyl/ethyl esters) obtained from long chain fatty acids derived from renewable lipid sources (e.g., rapeseed oil in Europe and soybean oil in the United States) by transesterification with methanol or ethanol (2,3). It should be mentioned that the presence of additional oxygenated compounds could reduce the formation of soot in diesel engines (4,5) but may also promote the formation of some toxic pollutants, such as aldehydes (6).

The need to develop more efficient, but cleaner, engines requires the development of validated detailed kinetic models for the oxidation of fuels. If such mechanisms start to be available for surrogates of gasoline and diesel fuel, there are few kinetic models for the oxidation of methyl and ethyl esters. Despite rapeseed and soybean oils are mainly composed of compounds containing more than 16 atoms of carbon, it is interesting to better understand the reactivity of the oxygenated part of these molecules by studying first a small chain methyl/ethyl ester. The first detailed modeling of the oxidation of methyl esters has been proposed by Fisher et al. (7) for methyl formate and methyl butanoate with validation using experimental results obtained in static reactors below 900 K (8). More recently, a mechanism of the oxidation of methyl butanoate has been proposed by Gaïl et al. (9) with validations over a wide range of operating conditions, including results obtained in a jet-stirred reactor from 800 to 1350 K (no significant conversion was obtained below 950 K), in a flow reactor, from 500 to 900 K (no significant conversion was obtained below 750 K) and in an opposed-flow diffusion flame. Metcalfe et al. (10) have experimentally and theoretically studied the high-temperature ignition of methyl butanoate and ethyl propanoate using their shock tube at temperatures between 1100 and 1670 K. The proposed model has recently been updated to simulate experimental results obtained in a jet-stirred reactor from 750 to 1100 K for ethyl propanoate (11). Dooley et al. (12) have studied the low-temperature ignition of methyl butanoate in their rapid compression machine over the temperature range 640–949 K. These authors have also proposed a model able to reproduce the rapid compression machine data, but also the measurements of Gail et al. 9 in a jet-stirred reactor, a flow reactor, and an opposed-flow diffusion flame. Walton et al. (13) have experimentally studied the ignition of methyl butanoate and ethyl propanoate using their rapid compression machine at temperatures between 935 and 1117 K and slightly modified the model proposed by Metcalfe et al. (10). Theoretical calculations were performed by Huynh and Violi (14) for some reactions of importance for the thermal decomposition of methyl butanoate and applied successfully by Faroq et al. (15) to model experimental data obtained behind reflected shock waves (temperatures from 1260 to 1653 K). Hayes and Burgess (16) made theoretical calculations for some reactions important in the oxidative decomposition of methyl butanoate. No data have been yet reported for ethyl butanoate.

The first purpose of this paper is to present new experimental data about the oxidation of small-saturated esters, including a comparative study of the ignition delay times of methyl and ethyl butanoate. A second objective is to describe new detailed kinetic models for the oxidation of these species generated using an automatic method and validated over a wide range of experimental conditions.

Experimental

This experimental study has been performed by using two different devices: a jet-stirred reactor and a shock tube. Methyl butanoate (99% pure) and ethyl butanoate (98% pure) were provided by Fluka (Saint Quentin Fallavier, France). Oxygen (99.5% pure) and argon and helium (both 99.995% pure) were supplied by Messer (Folschwiller, France).

Shock Tube

As the measurement of ignition delay times in the used shock tube has been described in several papers (17–20), the main features of this experimental device will just be recalled here. Autoignition delay times have been measured in a stainless steel shock tube; the reaction and the driver parts were, respectively, 400.6 and 89 cm in length and 7.8 and 12.82 cm in diameter and were separated by two terphane diaphragms. These diaphragms were ruptured by suddenly decreasing the pressure in the space separating them, that allowed us to keep the same pressure (5.3 bar) in the high-pressure part for all experiments. The driver gas was helium. The incident shock velocities were measured by four piezoelectric pressure transducers located along the reaction section (the distance between each transducer was 15 cm and the last one was located at 1 mm from the end-plate of the tube). The pressure P_5 and temperature T_5 of the test gas behind the reflected shock wave were derived from the values of the initial pressure (P_1) in the low-pressure section (ranging from 10 to 40 kPa) and of the incident shock velocity (V) by using ideal one-dimensional shock equations. The error on the temperature was estimated about 20 K.

The onset of ignition was detected by OH radical emission at 306 nm through a quartz window with a photomultiplier fitted with a monochromator at the end of the reaction part (the center of the window was located at 1 mm from the end-plate of the tube at the same place as the last pressure transducer). It is worth noting that the experimental OH emission at 306 nm is related to electronically excited OH* concentration.

Fresh reaction mixtures were prepared every day and mixed using a recirculation pump. Before each introduction of the reaction mixture (vacuum in low-pressure part obtained by a primary pump for a pressure around 1×10^{-3} kPa), the reaction section was flushed with pure argon and evacuated, to ensure the residual gas to be mainly argon.

Jet-Stirred Reactor

The oxidation of methyl butanoate was carried out in a jet-stirred reactor (internal volume about 92 cm^3) made of quartz and operated at a constant temperature and pressure. This type of spherical reactor is well adapted for kinetic studies because the gas phase inside the reactor has been proved to be well stirred and concentrations are homogeneous therein (21). It has already been used many times in our laboratory for studying the oxidation of organic compounds with satisfactory modeling of the obtained results (e.g., 22,23). The heating of the reactor was achieved by means of electrically insulated resistors directly coiled around the vessel. Temperature was measured by using a thermocouple located inside the reactor; reactants were preheated at a temperature close to the

reaction temperature. Corresponding residence time in the preheating section was approximately 1% of the total residence time.

The liquid fuel was contained in a glass vessel pressurized with helium. After each load of the vessel, helium bubbling and vacuum pumping were performed to remove oxygen traces dissolved in the liquid hydrocarbon fuel. The liquid reactant flow rate was controlled by using a liquid mass flow controller, mixed to the carrier gas, helium, and then evaporated by passing through a single pass heat exchanger whose temperature is set above the boiling point of the mixture. Carrier gas and oxygen flow rates were controlled by gas mass flow controllers located before the mixing chamber. The fuel/oxygen/helium mixtures were premixed prior the introduction into the reactor.

Owing to the formation of compounds, which were either gaseous or liquid at room temperature, the analyses of the products leaving the reactor were performed in two steps:

- For the analysis of heavy products, the outlet flow was directed toward a trap maintained at liquid nitrogen temperature during a determined period of time. The use of helium instead of nitrogen as diluent prevents trapping of the carrier gas and has a negligible effect on the obtained results compared to the use of nitrogen. At the end of this period (typically 10 min), the trap was removed and, after the addition of acetone and of an internal standard (*n*-octane), progressively heated up. When the temperature of the trap was close of 273 K the mixture was poured into a small bottle and then injected by an autosampler in a gas chromatograph with flame ionization detection (FID) for quantification. The column used for the separation was a HP-1 capillary column with helium as carrier gas. Calibrations were performed by analyzing a range of solutions containing known amounts of *n*-octane and of the species to be analyzed. Species heavier than methyl butanoate have not been analyzed.

- Oxygen, carbon oxides, and C_1–C_2 hydrocarbons were analyzed online by a chromatograph fitted with both thermal conductivity detector (TCD) for oxygen and carbon oxides detection and FID for methane and C_2 hydrocarbons detection and using a CARBOSPHERE packed column with helium as carrier gas. Species identification and calibration was realized by injection of gaseous standard mixtures provided by Air Liquide (Metz, France). Using helium as carrier gas both in the reactor and in this gas chromatograph facilitates the quantification of oxygen.

Water, formaldehyde, hydrogen, and C_3–C_4 hydrocarbons have not been analyzed. Calculated uncertainties on the species quantifications were about ±5% with the online analysis of oxygen and C_1–C_2 hydrocarbons and about ±10% for the analysis of other species.

It is worth noting that important problems were encountered in performing these experiments due to reactions between methyl butanoate and seals inside the flowmeters. Methyl butanoate dissolved both Kalrez and Viton seals damaging the flowmeters and producing leakages. Since experiments were only performed with well functioning flowmeters, these problems have not affected the present measurements, but they have prevented us from testing more experimental conditions.

Results

Shock Tube

This study was performed under the following experimental conditions after the reflected shock wave:

- temperature range from 1280 to 1990 K,
- pressure maintained around 8 atm, ranging from 7.6 to 9.1 atm, and
- argon/ester/oxygen mixtures corresponding to three different equivalence ratios (ϕ = 0.25, 1 and 2) and to three different concentrations of esters (0.417 (only in the case of ethyl butanoate), 0.5 and 1%) and allowing delay times from 5 up to 700 μs to be obtained.

Figure 1 presents the record of the signal of the last pressure transducer and of the OH emission for a typical experiment in the case of ethyl butanoate. The pressure profile displayed three rises, which were due to the incident shock wave, 1; the reflected shock wave, 2; and the ignition. This last pressure rise is sharp enough for determining the delay time, while the rise of OH emission, 3, is much steeper and allows the delay time to be known with an accuracy better than 10%. The ignition delay time (τ) was defined as the time interval between the pressure rise measured by the last pressure transducer due to the arrival of the reflected shock wave and the rise of the optical signal by the photomultiplier up to 10% of its maximum value as shown in Figure 1. As shown in Figure 1, all the obtained pressure signals display a slight rise prior to ignition, even in the lowest temperature cases. As this rise is reproduced by modeling, it is probably more due to kinetics than to nonideal shock tube effects or premature ignition. Note that this rise was not usually observed when studying other hydrocarbons (e.g., 19,20).

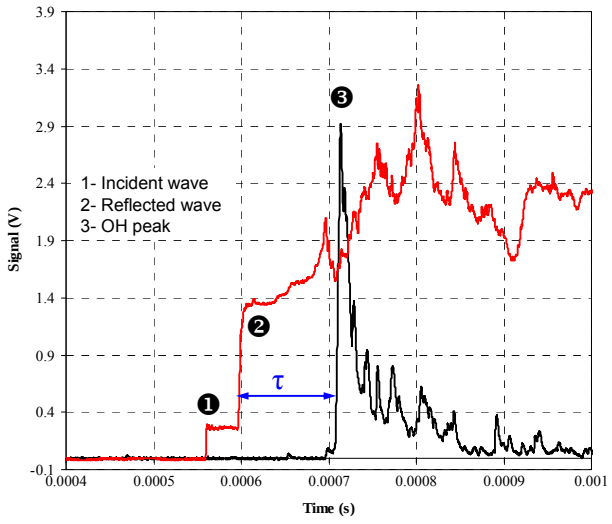

Figure 1. Typical experimental profiles of pressure and OH* emission in the case of ethyl butanoate.

Tables I and II present the complete set of experimental conditions and measurements performed in this study for methyl butanoate and ethyl butanoate, respectively. We usually consider that the range of ignition delay times that can be measured in this shock tube while maintaining ideal conditions (adiabaticity for long ignition delay times and reasonable uncertainties for short ignition

delay times) is between 10 and 1500 µs. However we present here a few points with ignition delay times shorter than 10 µs and then with a larger uncertainty.

Table 1. Mixture Compositions, Shock Conditions, and Ignition Delay Times for Methyl Butanoate.

P_1 (kPa)	P_5 (atm)	V (m/s)	τ (µs)	T_5 (K)	P_1 (kPa)	P_5 (atm)	V (m/s)	τ (µs)	T_5 (K)
ϕ = 1; X_{MB} = 1%; X_{02} = 6.5%; X_{Ar} = 92.5%					ϕ = 1; X_{MB} = 0.5%; X_{02} = 3.25%; X_{Ar} = 96.25%				
26.7	8.5	803	98.2	1375	32.0	9.2	789	153	1402
30.0	8.3	764	544	1265	30.7	8.6	782	135	1380
29.3	8.4	775	424	1296	30.7	8.2	769	317	1341
29.3	9.0	794	216	1349	29.5	8.5	791	100	1408
29.0	8.8	789	240	1335	28.0	8.7	812	47.2	1474
28.4	8.1	774	367	1293	28.0	8.6	807	86.9	1458
28.0	9.1	808	107	1389	27.3	8.1	799	57.9	1433
24.0	8.0	817	66.0	1415	26.7	8.5	819	38.5	1496
23.3	8.6	845	26.6	1497	25.5	8.7	839	21.1	1563
22.7	8.4	846	19.0	1500	24.0	8.0	831	33.3	1536
22.6	8.3	844	24.1	1494	23.2	8.2	849	22.0	1593*
21.3	7.8	845	28.4	1497	22.8	8.4	860	13.5	1631
20.0	7.9	867	11.9	1564	21.3	8.0	865	10.2	1648
20.0	*8.2*	*878*	*6.0*	*1598*	*20.7*	*7.8*	*870*	*7.2*	*1665*
–	–	–	–	–	*20.0*	*8.0*	*886*	*5.3*	*1718*
ϕ = 0.25; X_{MB} = 0.5%; X_{02} = 13%; X_{Ar} = 86.5%					ϕ = 2; X_{MB} = 0.5%; X_{02} = 1.625%; X_{Ar} 97.875%				
30.7	8.5	776	340	1290	25.3	8.3	828	93.0	1540
31.1	8.8	780	309	1302	24.0	8.7	858	62.1	1640
30.4	8.5	777	271	1294	22.7	8.2	858	56.5	1639
30.0	8.7	787	130	1320	22.7	8.3	861	52.3	1650
29.3	8.8	797	98.9	1350	21.3	7.9	863	46.9	1657
28.0	8.2	792	88.9	1335	20.7	8.0	876	24.0	1702
28.7	8.7	801	63.7	1362	18.7	7.8	902	16.2	1792
27.8	8.7	807	36.2	1380	19.3	8.1	902	15.6	1792
26.7	8.3	807	34.8	1380	18.2	7.7	905	14.4	1804
28.0	9.0	816	31.9	1405	20.0	8.2	897	13.9	1774
27.0	8.9	823	25.8	1426	*17.4*	*7.7*	*925*	*9.1*	*1875*
25.3	8.1	815	23.4	1402	*16.7*	*7.7*	*936*	*5.9*	*1915*
26.0	8.5	820	20.8	1417	–	–	–	–	–
25.3	8.2	817	16.4	1408	–	–	–	–	–
24.0	8.1	830	11.7	1446	–	–	–	–	–
24.9	8.0	823	11.4	1426	–	–	–	–	–
24.0	*8.2*	*835*	*9.4*	*1461*	–	–	–	–	–
23.3	*8.0*	*835*	*9.1*	*1461*	–	–	–	–	–
24.7	*8.4*	*834*	*7.5*	*1458*	–	–	–	–	–
21.3	*7.8*	*853*	*5.7*	*1515*	–	–	–	–	–

[a] P_1 is the pressure of the mixture before the shock, V is the velocity of the incident wave, P_5 and T_5 are pressure and temperature behind the reflected shock wave, and τ is the ignition delay time. Italic corresponds to ignition delay times below 10 µs and then to a larger uncertainty.

Table II. Mixture Compositions, Shock Conditions, and Ignition Delay Times for Ethyl Butanoate.

P_1 (kPa)	P_5 (atm)	V (m/s)	τ (μs)	T_5 (K)	P_1 (kPa)	P_5 (atm)	V (m/s)	τ (μs)	T_5 (K)
ϕ = 1; X_{EB} = 1%; X_{02} = 8%; X_{Ar} = 91%					ϕ = 1; X_{EB} = 0.5%; X_{02} = 4%; X_{Ar} = 95.5%				
27	8.2	784	321.5	1296	29.3	8.5	788	111.7	1385
29.3	7.8	784	259	1301	27.9	8.2	790	97	1390
28.6	8.9	790	311	1313	27.3	8.2	797	71.3	1411
28	9.2	804	114	1352[a]	26.6	8.3	807	37.8	1442
25.3	8.3	806	84.3	1358	25.9	8.2	813	36.5	1459
23.3	7.9	814	34.4	1378	24.6	7.9	815	25.5	1468
24.6	8.4	816	56.4	1384	25.3	8.5	831	26.7	1516
26	9	822	42.3	1401	22.6	7.8	835	15.5	1530
24	8.5	826	15.2	1412	23.9	8.2	836	13.3	1533
22.6	8.3	837	16.6	1443	23.3	8.2	843	12.4	1555
23	8.7	848	11	1474	–	–	–	–	–
ϕ = 1; X_{EB} = 0.42%; X_{02} = 3.33%; X_{Ar} = 96.25%					ϕ = 0.25; X_{EB} = 0.5%; X_{02} = 16%; X_{Ar} = 83.5%				
9.6	8.5	758	1485	1307	29.9	8.7	783	188.6	1282
2	8.7	785	123.4	1388	29.3	8.5	785	101.4	1288
42.8	8.9	786	153.7	1393	28	8.4	794	106.7	1311
2.2	9.2	788	191.1	1398	27.7	8.5	799	75.6	1325
15.2	8.7	798	87.2	1429	27.4	8.7	810	36	1356
12.6	8.4	802	59.4	1441	26.6	8.8	820	20.3	1386
5.6	7.9	813	31.9	1475	23.4	7.8	821	13.2	1386
4.6	8.4	820	23	1498	25.3	8.4	823	14.5	1393
34.4	8.6	822	22.3	1505	24.6	8.5	833	11.4	1422
11.2	8.1	834	10.7	1543	*23.9*	*8.3*	*833*	*6.8*	*1423*
41.4	7.8	840	10	1562	*22.6*	*8.1*	*842*	*5.3*	*1448*
7.5	*8.1*	*843*	*5.5*	*1573*	–	–	–	–	–
15	*8.6*	*843*	*9.8*	*1574*	–	–	–	–	–
ϕ = 2; X_{EB} = 0.5%; X_{02} = 2%; X_{Ar} = 97.5%									
25.5	8.6	830	88.3	1532	21.3	7.9	859	47.1	1628
24.4	8.4	837	58	1555	19.3	7.9	894	14.9	1743
22.3	7.7	840	40.4	1563	16.6	7.3	914	10.8	1814
22.3	7.8	840	65.5	1566	*17.3*	*7.6*	*915*	*9.7*	*1816*
22.6	7.9	841	39.4	1569	*16.4*	*7.6*	*935*	*6.6*	*1888*
23.3	8.1	842	47.3	1571	–	–	–	–	–

[a] P_1 is the pressure of the mixture before the shock, V is the velocity of the incident wave, P_5 and T_5 are pressure and temperature behind the reflected shock wave, and τ is the ignition delay time. Italic corresponds to ignition delay times below 10 μs and then to a larger uncertainty.

[b] Conditions of the signals displayed in Figure 1.

Figures 2 and 3 present the experimental results obtained for the ignition of methyl butanoate and ethyl butanoate, respectively. Figures 2a and 3a correspond to mixtures containing 0.5% of ester, for three equivalent ratios. Figures 2b and 3b display the experimental results obtained for different ester concentrations with stoichiometric mixtures. These results show that in each case, ignition delay times increase when equivalence ratio increases and decrease when dilution decreases.

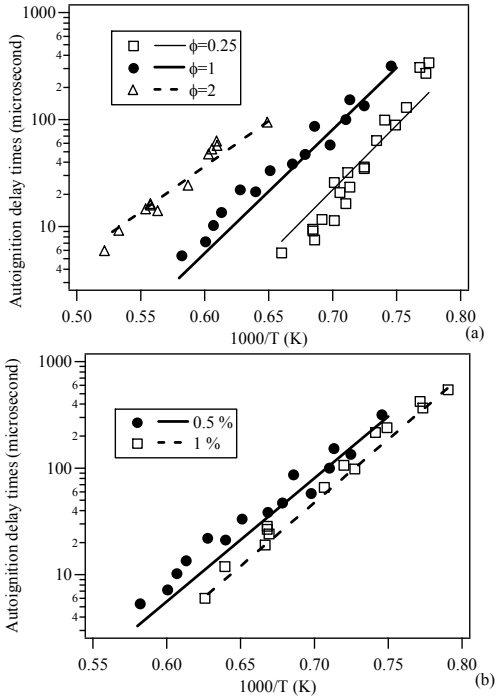

Figure 2. Ignition delay times of methyl butanoate in a shock tube for (a) equivalence ratios of 0.25, 1, and 2 and a concentration of ester of 0.5% and (b) an equivalence ratio of 1 and concentrations of ester of 0.5% and 1%. Points correspond to experimental results and lines to simulations.

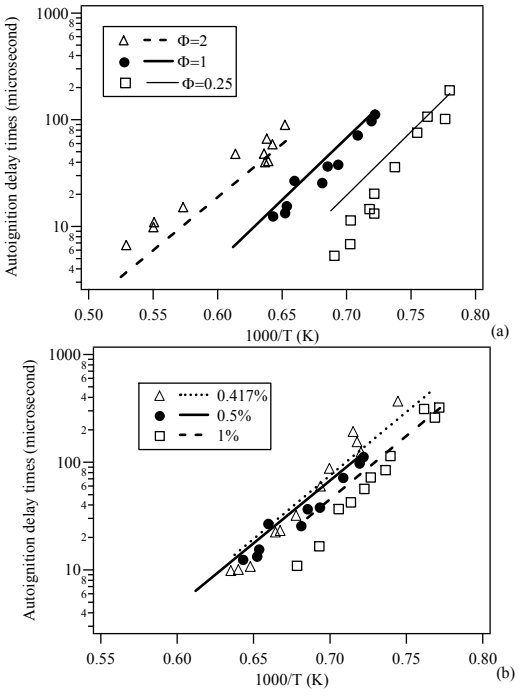

Figure 3. Ignition delay times of ethyl butanoate in a shock tube for (a) equivalence ratios of 0.25, 1, and 2 and a concentration of ester of 0.5% and (b) an equivalence ratio of 1 and concentrations of ester of 0.417%, 0.5%, and 1%. Points correspond to experimental results and lines to simulations.

The two series corresponding to stoichiometric mixtures and a concentration of ester of 0.5% for methyl butanoate and 0.417% for ethyl butanoate have been made to obtain a direct comparison between both compounds with the same concentration of carbon atoms and the same C/O ratio. Figure 4 displays these results and shows a very small difference of reactivity between both esters. The ignition delay times for ethyl butanoate are slightly lower than for methyl butanoate above 1600 K. The results obtained by Metcalfe et al. (10) concerning the ignition of methyl butanoate and ethyl propanoate also show the ethyl ester to be the more reactive, but the difference in reactivity is more important at low temperature.

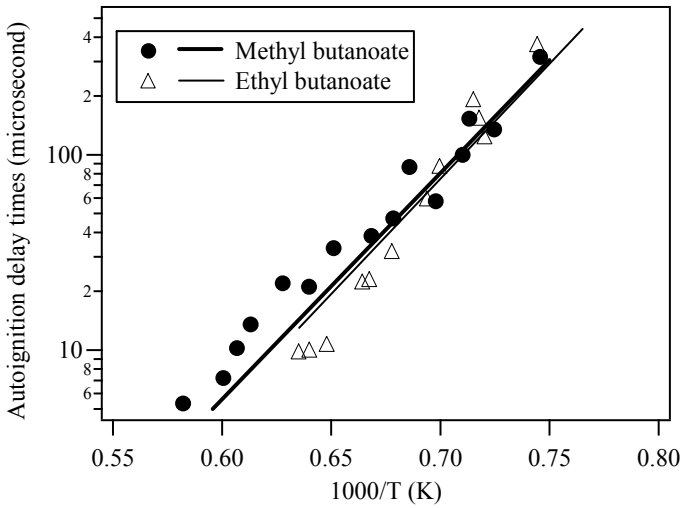

Figure 4. Comparison between autoignition delay times of methyl and ethyl butanoate in a shock tube for an equivalence ratio of 1 and a concentration of ester of 0.5% for methyl butanoate and of 0.417% for ethyl butanoate (corresponding to the same concentration of atoms of carbon). Points correspond to experimental results and lines to simulations.

For organic compound/oxygen/argon mixtures, the determination of power dependences is often proposed from the overall statistical correlation between τ and the gas concentrations:

$$\tau = A \exp(E/RT) [OC]^a [O_2]^b [Ar]^c$$

where A is the preexponential factor, E the apparent "activation energy," and R the gas constant (24). For a restricted range of pressure and temperature, a, b, and c are usually constant. Such a statistical correlation has been derived from the present experiments, but since the mole fraction of argon had limited variations under the different initial conditions (from 83.5% to 97.785%) and seems not to affect the delay times, it was chosen to keep c = 0. A multilinear regression gave the following relationships, with the concentrations behind the reflected shock wave in mol cm^{-3} and E in cal/mol:

- For methyl butanoate (MB):

$$\tau(s) = 2.54 \times 10^{-20} \exp(55580/RT) [MB]^{0.140} [O_2]^{-1.45}$$

- For ethyl butanoate (EB):

$\tau(s) = 1.88x10^{-20} \exp(57540/RT) [EB]^{0.250} [O_2]^{-1.52}$

These statistical correlations show a strong negative O_2 power dependence, whereas the fuel power dependence is very small. Previous work with other organic compounds has also shown large negative O_2 power dependence and much smaller positive fuel power dependence (19,25). The apparent activation energy is slightly larger for the ethyl ester compared to the methyl one. This difference is in agreement with what can been seen in Figure 4.

Jet-Stirred Reactor

Table III presents the complete set of experimental conditions and measurements performed in this study for methyl butanoate. These results are displayed in Figures 5 to 7. As shown in Figure 5, the oxidation of methyl butanoate leads to the formation of similar amounts of two unsaturated esters, namely methyl crotonate (methyl 2-butenoate; Figure 5b) and methyl acrylate (methyl propenoate; Figure 5c). Concerning the oxygenated products displayed in Figure 6, the formation of carbon dioxide (Figure 6c) is larger than what should be obtained only from the reactions of carbon monoxide (Figure 6b) at the low temperatures used in this study, i.e., 800 and 850 K. Among C_1–C_2 hydrocarbons (Figure 7), methane (Figure 7a) and ethylene (Figure 7b) are the most abundant ones, whereas the levels of acetylene and ethane (Figure 7c) are lower than 30 ppm.

Table 3. Experimental Results Obtained in a Jet-Stirred Reactor for Methyl Butanoate.

	Residence Times (s)																
	1.5		3			4.5		6			7.5			9			
Compounds	**Mole Fraction**																
	ϕ = 0.5; X_{MB} = 2%; X_{02} = 26%; X_{He} = 72%; T = 800 K																
O_2	2.57×10^{-1}	2.55×10^{-1}	2.10×10^{-1}	2.09×10^{-1}	2.09×10^{-1}	1.94×10^{-1}	1.94×10^{-1}	1.95×10^{-1}	1.89×10^{-1}	1.88×10^{-1}	1.89×10^{-1}	1.87×10^{-1}	1.82×10^{-1}	1.83×10^{-1}	1.87×10^{-1}	1.83×10^{-1}	1.84×10^{-1}
CO	1.39×10^{-4}	1.45×10^{-4}	4.59×10^{-3}	5.26×10^{-3}	5.38×10^{-3}	1.78×10^{-2}	1.66×10^{-2}	1.55×10^{-2}	2.43×10^{-2}	2.51×10^{-2}	2.43×10^{-2}	2.81×10^{-2}	2.99×10^{-2}	2.99×10^{-2}	3.65×10^{-2}	3.66×10^{-2}	3.53×10^{-2}
CO_2	–	2.92×10^{-4}	5.02×10^{-4}	1.50×10^{-3}	1.81×10^{-3}	3.54×10^{-3}	4.61×10^{-3}	2.97×10^{-3}	5.59×10^{-3}	6.02×10^{-3}	5.51×10^{-3}	6.95×10^{-3}	7.65×10^{-3}	6.96×10^{-3}	1.14×10^{-2}	1.04×10^{-2}	9.28×10^{-3}
CH_4	6.50×10^{-5}	6.41×10^{-5}	6.15×10^{-4}	6.70×10^{-4}	7.01×10^{-4}	1.57×10^{-3}	1.55×10^{-3}	1.40×10^{-3}	1.95×10^{-3}	2.03×10^{-3}	1.99×10^{-3}	2.05×10^{-3}	2.14×10^{-3}	2.11×10^{-3}	2.50×10^{-3}	2.44×10^{-3}	2.38×10^{-3}
C_2H_2	–	–	4.96×10^{-7}	6.71×10^{-7}	6.83×10^{-7}	3.31×10^{-6}	2.79×10^{-6}	3.45×10^{-6}	5.31×10^{-6}	5.00×10^{-6}	5.11×10^{-6}	6.02×10^{-6}	5.75×10^{-6}	6.17×10^{-6}	6.81×10^{-6}	6.56×10^{-6}	5.92×10^{-6}
C_2H_4	8.75×10^{-5}	8.09×10^{-5}	1.58×10^{-3}	1.71×10^{-3}	1.78×10^{-3}	3.53×10^{-3}	3.48×10^{-3}	3.20×10^{-3}	4.02×10^{-3}	4.13×10^{-3}	4.11×10^{-3}	4.02×10^{-3}	4.08×10^{-3}	4.02×10^{-3}	4.46×10^{-3}	4.36×10^{-3}	4.25×10^{-3}
C_2H_6	5.60×10^{-7}	7.81×10^{-7}	8.88×10^{-6}	1.04×10^{-5}	1.03×10^{-5}	2.05×10^{-5}	2.11×10^{-5}	1.82×10^{-5}	2.34×10^{-5}	2.44×10^{-5}	2.38×10^{-5}	2.18×10^{-5}	2.32×10^{-5}	2.25×10^{-5}	2.61×10^{-5}	2.44×10^{-5}	2.43×10^{-5}
Methyl acrylate	7.66×10^{-5}	7.82×10^{-5}	8.67×10^{-4}	8.93×10^{-4}	9.12×10^{-4}	1.29×10^{-3}	1.30×10^{-3}	1.32×10^{-3}	1.31×10^{-3}	1.29×10^{-3}	1.30×10^{-3}	1.19×10^{-3}	1.18×10^{-3}	1.18×10^{-3}	1.19×10^{-3}	1.20×10^{-3}	1.09×10^{-3}
Methyl crotonate	7.75×10^{-5}	7.61×10^{-5}	7.39×10^{-4}	7.68×10^{-4}	7.70×10^{-4}	8.81×10^{-4}	8.92×10^{-4}	9.03×10^{-4}	8.11×10^{-4}	7.87×10^{-4}	8.05×10^{-4}	7.10×10^{-4}	6.98×10^{-4}	7.23×10^{-4}	6.99×10^{-4}	7.03×10^{-4}	6.61×10^{-4}
Methyl butanoate	1.94×10^{-2}	1.72×10^{-2}	1.50×10^{-2}	1.56×10^{-2}	1.51×10^{-2}	1.02×10^{-2}	1.04×10^{-2}	1.04×10^{-2}	8.14×10^{-3}	7.87×10^{-3}	8.06×10^{-3}	6.50×10^{-3}	6.42×10^{-3}	6.59×10^{-3}	5.83×10^{-3}	5.92×10^{-3}	5.56×10^{-3}
ϕ = 1; X_{MB} = 2%; X_{02} = 13%; X_{He} = 85%; T = 850 K																	
O_2	9.77×10^{-2}	9.66×10^{-2}	8.41×10^{-2}	8.29×10^{-2}	8.84×10^{-2}	7.86×10^{-2}	7.37×10^{-2}	8.07×10^{-2}	7.51×10^{-2}	7.40×10^{-2}	8.50×10^{-2}	8.19×10^{-2}	$8.51 \times 10–^{2}$	7.24×10^{-2}	6.63×10^{-2}	6.20×10^{-2}	–
CO	1.02×10^{-2}	1.09×10^{-2}	3.06×10^{-2}	2.92×10^{-2}	2.90×10^{-2}	3.64×10^{-2}	3.73×10^{-2}	3.78×10^{-2}	4.36×10^{-2}	4.06×10^{-2}	4.20×10^{-2}	4.09×10^{-2}	4.28×10^{-2}	4.45×10^{-2}	5.06×10^{-2}	5.11×10^{-2}	–
CO_2	2.10×10^{-3}	2.19×10^{-3}	7.30×10^{-3}	8.41×10^{-3}	6.69×10^{-3}	1.07×10^{-2}	1.14×10^{-2}	1.01×10^{-2}	1.26×10^{-2}	1.18×10^{-2}	1.37×10^{-2}	1.21×10^{-2}	1.44×10^{-2}	1.39×10^{-2}	1.75×10^{-2}	1.99×10^{-2}	–

	Residence Times (s)															
	1.5		3		4.5			6			7.5			9		
Compounds	**Mole Fraction**															
	ϕ = 0.5; X_{MB} = 2%; X_{O2} = 26%; X_{He} = 72%; T = 800 K															
CH_4	2.78×10^{-3}	2.87×10^{-3}	4.82×10^{-3}	4.75×10^{-3}	4.66×10^{-3}	5.01×10^{-3}	5.08×10^{-3}	5.20×10^{-3}	5.47×10^{-3}	5.56×10^{-3}	5.07×10^{-3}	5.33×10^{-3}	5.50×10^{-3}	5.21×10^{-3}	5.63×10^{-3}	5.75×10^{-3}	–
C_2H_2	2.49×10^{-6}	2.87×10^{-6}	9.76×10^{-6}	9.37×10^{-6}	1.08×10^{-5}	1.17×10^{-5}	1.16×10^{-5}	1.24×10^{-5}	1.30×10^{-5}	1.27×10^{-5}	1.28×10^{-5}	1.25×10^{-5}	1.29×10^{-5}	1.28×10^{-5}	1.34×10^{-5}	1.32×10^{-5}	–
C_2H_4	4.27×10^{-3}	4.45×10^{-3}	7.77×10^{-3}	7.70×10^{-3}	7.66×10^{-3}	8.04×10^{-3}	7.99×10^{-3}	8.27×10^{-3}	8.44×10^{-3}	8.51×10^{-3}	7.93×10^{-3}	8.13×10^{-3}	8.42×10^{-3}	7.85×10^{-3}	8.31×10^{-3}	8.41×10^{-3}	–
C_2H_6	1.06×10^{-4}	1.44×10^{-4}	1.90×10^{-4}	1.90×10^{-4}	1.85×10^{-4}	1.76×10^{-4}	1.72×10^{-4}	1.80×10^{-4}	1.81×10^{-4}	1.90×10^{-4}	1.63×10^{-4}	1.75×10^{-4}	1.81×10^{-4}	1.60×10^{-4}	1.70×10^{-4}	1.76×10^{-4}	–
Methyl acrylate	1.09×10^{-3}	1.07×10^{-3}	1.00×10^{-3}	1.09×10^{-3}	1.09×10^{-3}	8.05×10^{-4}	8.23×10^{-4}	–	7.23×10^{-4}	7.24×10^{-4}	7.37×10^{-4}	7.28×10^{-4}	7.18×10^{-4}	6.79×10^{-4}	4.92×10^{-4}	4.84×10^{-4}	3.85×10^{-4}
Methyl crotonate	2.86×10^{-4}	2.75×10^{-4}	2.50×10^{-4}	2.50×10^{-4}	2.23×10^{-4}	1.71×10^{-4}	1.63×10^{-4}	1.45×10^{-4}	1.36×10^{-4}	1.40×10^{-4}	1.28×10^{-4}	1.42×10^{-4}	1.38×10^{-4}	1.34×10^{-4}	8.70×10^{-5}	8.51×10^{-5}	7.13×10^{-5}
Methyl butanoate	1.12×10^{-2}	1.10×10^{-2}	6.53×10^{-3}	6.60×10^{-3}	5.86×10^{-3}	4.24×10^{-3}	4.13×10^{-3}	3.49×10^{-3}	3.47×10^{-3}	3.51×10^{-3}	3.56×10^{-3}	3.38×10^{-3}	3.32×10^{-3}	3.15×10^{-3}	2.06×10^{-3}	2.11×10^{-3}	1.74×10^{-3}

[a] *Note:* Methyl acrylate: $C_4H_6O_2$; methyl crotonate: $C_5H_8O_2$; methyl butanoate: $C_5H_{10}O_2$. Each value in each column corresponds to a separate run.

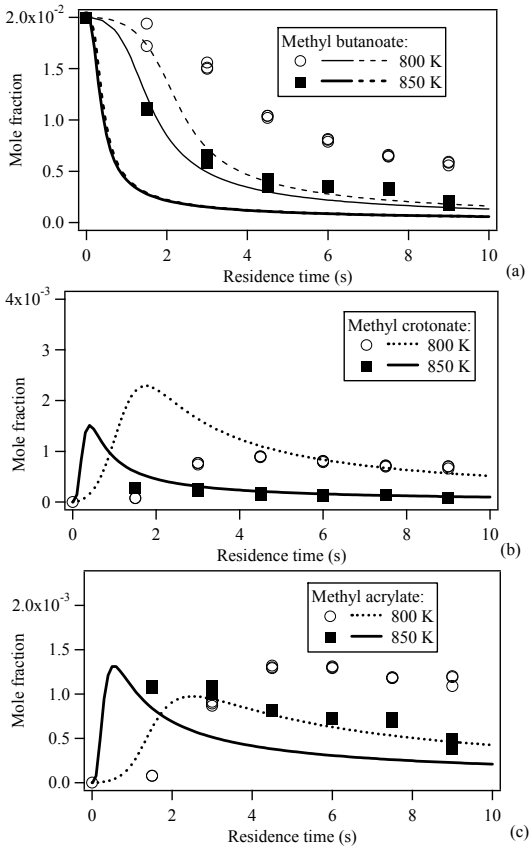

Figure 5. Time evolution profiles for the consumption of the ester and the formation of methyl crotonate and methyl acrylate measured during the oxidation of methyl butanoate in a jet-stirred reactor at 800 K for an equivalence ratio of 0.5 and at 850 K for an equivalence ratio of 1. Points correspond to experimental results, full lines to simulations with the complete mechanism, and dotted lines to simulations with a mechanism without the low-temperature reactions.

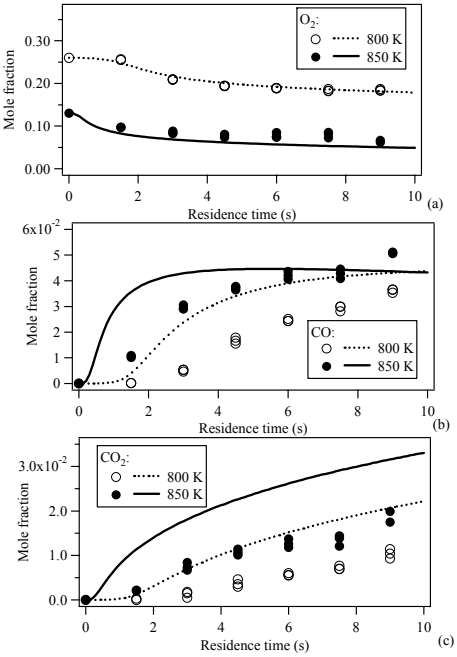

Figure 6. Time evolution profiles for the consumption of oxygen and the formation of carbon oxides measured during the oxidation of methyl butanoate in a jet-stirred reactor at 800 K for an equivalence ratio of 0.5 and at 850 K for an equivalence ratio of 1. Points correspond to experimental results and lines to simulations.

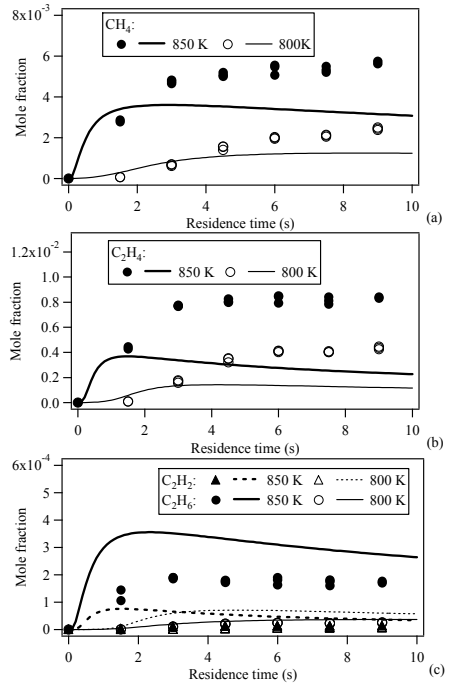

Figure 7. Time evolution profiles for the formation of C_1–C_2 hydrocarbons measured during the oxidation of methyl butanoate in a jet-stirred reactor at 800 K for an equivalence ratio of 0.5 and at 850 K for an equivalence ratio of 1. Points correspond to experimental results and lines to simulations.

Description of the Detailed Kinetic Model

The detailed chemical kinetic reaction mechanisms presented here have been developed using EXGAS software. As the use of EXGAS to model the oxidation of alkanes and ethers has already been extensively described (23,26–29), we will recall here only its main features. However, we will provide more detail on the reactions and rate constants specific to the two small esters studied here.

General Features of EXGAS

The system provides reaction mechanisms made of three parts that are used together:

- A comprehensive primary mechanism in which the only molecular reactants considered are the initial organic compounds and oxygen (see Table IV in the case of methyl butanoate). For modeling results obtained above 1000 K, the mechanism can include only high-temperature reactions, which are in the case of saturated hydrocarbons:
- unimolecular initiations involving the breaking of a C-C bond,
- bimolecular initiations with oxygen to produce alkyl (R•) and hydroperoxy (•OOH) radicals,
- isomerizations of alkyl radicals involving a cyclic transition state and the transfer of an H-atom,
- decompositions of radicals by β-scission involving the breaking of C-C, C-O or C-H bonds for all types of radicals,
- oxidations of alkyl radicals with O_2 to form alkenes and $\bullet HO_2$ radicals,
- metatheses between radicals and the initial reactants (H-abstractions), and
- combinations and dismutations of radicals.

Table IV. Primary Mechanism for the Oxidation of Methyl Butanoate.

Reactions	*A*	*n*	E_a	Equation Number
Unimolecular initiations				
$C_5H_{10}O_2S \rightarrow {}^{\bullet}CH_2CH_2C(=O)OCH_3 + {}^{\bullet}CH_3$	1.7×10^{17}	0.0	86,911	(1)
$C_5H_{10}O_2S \rightarrow {}^{\bullet}CH_2C(=O)OCH_3 + {}^{\bullet}C_2H_5$	3.8×10^{16}	0.0	81,705	(2)
$C_5H_{10}O_2S \rightarrow CH_3O^{\bullet}CO + n{C_3H}^{\bullet}{}_7$	7.9×10^{16}	0.0	92,781	(3)
$C_5H_{10}O_2S \rightarrow CH_3O^{\bullet} + {C_3H}^{\bullet}{}_7CO$	1.5×10^{16}	0.0	96,856	(4)
$C_5H_{10}O_2S \rightarrow {}^{\bullet}CH_3 + C_3H_7C(=O)O^{\bullet}$	3.5×10^{15}	0.0	84,439	(5)
Bimolecular initiations				
$C_5H_{10}O_2S + O_2 \rightarrow HO^{\bullet}{}_2 + {}^{\bullet}CH_2C_2H_4C(=O)OCH_3$	2.1×10^{13}	0.0	53,030	(6)
$C_5H_{10}O_2S + O_2 \rightarrow HO^{\bullet}{}_2 + C_3H_7C(=O)OCH^{\bullet}{}_2$	2.1×10^{13}	0.0	51,130	(7)
$C_5H_{10}O_2S + O_2 \rightarrow HO^{\bullet}{}_2 + C_2H^{\bullet}{}_5CHC(=O)OCH_3$	1.4×10^{13}	0.0	46,508	(8)
$C_5H_{10}O_2S + O_2 \rightarrow HO^{\bullet}{}_2 + CH^{\bullet}{}_3CHCH_2C(=O)OCH_3$	1.4×10^{13}	0.0	50,586	(9)
Additions with oxygen				
$n{C_3H}^{\bullet}{}_7 + O_2 = C_3H_7(OO^{\bullet})$	9.0×10^{18}	−2.5	0	(10)
$n{C_4H}^{\bullet}{}_9 + O_2 = C_4H_9(OO^{\bullet})$	9.0×10^{18}	−2.5	0	(11)
${}^{\bullet}CH_2C_2H_4C(=O)OCH_3 + O_2 = CH_2(OO^{\bullet})C_2H_4C(=O)OCH_3$	9.0×10^{18}	−2.5	0	(12)
$C_3H_7C(=O)OCH^{\bullet}{}_2 + O_2 = C_3H_7C(=O)OCH2(OO^{\bullet})$	1.0×10^{18}	−2.5	0	(13)
$C_2H^{\bullet}{}_5CHC(=O)OCH_3 + O_2 = C_2H_5CH(OO^{\bullet})C(=O)OCH_3$	1.0×10^{19}	−2.5	0	(14)
$CH^{\bullet}{}_3CHCH_2C(=O)OCH_3 + O_2 = CH_3CH(OO^{\bullet})CH_2C(=O)OCH_3$	1.7×10^{19}	−2.5	0	(15)
${}^{\bullet}CH_2C(=O)OCH_3 + O_2 = CH_2(OO^{\bullet})C(=O)OCH_3$	1.0×10^{18}	−2.5	0	(16)
$CH^{\bullet}{}_3CHCH_2(OOH) + O_2 = CH_3CH(OO^{\bullet})CH_2(OOH)$	1.7×10^{19}	−2.5	0	(17)
${}^{\bullet}CH_2C_2H_4(OOH) + O_2 = CH_2(OO^{\bullet})C_2H_4(OOH)$	9.0×10^{18}	−2.5	0	(18)
$C_2H^{\bullet}{}_5CHCH_2(OOH) + O_2 = C_2H_5CH(OO^{\bullet})CH_2(OOH)$	1.8×10^{19}	−2.5	0	(19)

Reactions	A	n	E_a	Equation Number
$CH^{\bullet}{}_3CHC_2H_4(OOH) + O_2 = (OOH)C_2H_4CH(OO^{\bullet})CH_3$	1.7×10^{19}	−2.5	0	(20)
$^{\bullet}CH_2C_3H_6(OOH) + O_2 = CH_2(OO^{\bullet})C_3H_6(OOH)$	9.0×10^{18}	−2.5	0	(21)
$CH_2(OOH)^{\bullet}CHCH_2C(=O)OCH_3 + O_2 = CH_2(OOH)CH_2CH(OO^{\bullet})C(=O)OCH_3$	1.8×10^{19}	−2.5	0	(22)
$CH_2(OOH)CH^{\bullet}{}_2CHC(=O)OCH_3 + O_2 = CH_2(OOH)CH_2CH(OO^{\bullet})C(=O)OCH_3$	1.0×10^{19}	−2.5	0	(23)
$CH_3C(=O)OCH^{\bullet}{}_2 + O_2 = CH_3C(=O)OCH_2(OO^{\bullet})$	1.0×10^{18}	−2.5	0	(24)
$C_2H^{\bullet}{}_5CHC(=O)OCH_2(OOH) + O_2 = C_2H_5CH(OO^{\bullet})C(=O)OCH_2(OOH)$	1.0×10^{19}	−2.5	0	(25)
$CH^{\bullet}{}_3CHCH_2C(=O)OCH_2(OOH) + O_2 = CH_3CH(OO^{\bullet})CH_2C(=O)OCH_2(OOH)$	1.7×10^{19}	−2.5	0	(26)
$CH^{\bullet}{}_3CHCH(OOH)C(=O)OCH_3 + O_2 = CH_3CH(OO^{\bullet})CH(OOH)C(=O)OCH_3$	9.5×10^{18}	−2.5	0	(27)
$^{\bullet}CH_2CH_2CH(OOH)C(=O)OCH_3 + O_2 = CH_2(OO^{\bullet})CH_2CH(OOH)C(=O)OCH_3$	9.0×10^{18}	−2.5	0	(28)
$C_2H_5CH(OOH)C(=O)OCH^{\bullet}{}_2 + O_2 = C_2H_5CH(OOH)C(=O)OCH_2(OO^{\bullet})$	1.0×10^{18}	−2.5	0	(29)
$^{\bullet}CH_2CH(OOH)CH_2C(=O)OCH_3 + O_2 = CH_2(OO^{\bullet})CH(OOH)CH_2C(=O)OCH_3$	1.5×10^{18}	−2.5	0	(30)
$CH_3CH(OOH)^{\bullet}CHC(=O)OCH_3 + O_2 = CH_3CH(OOH)CH(OO^{\bullet})C(=O)OCH_3$	2.5×10^{18}	−2.5	0	(31)
$CH_3CH(OOH)CH_2C(=O)OCH^{\bullet}{}_2 + O_2 = CH_3CH(OOH)CH_2C(=O)OCH_2(OO^{\bullet})$	1.0×10^{18}	−2.5	0	(32)
$C_3H^{\bullet}{}_7CH(OOH) + O_2 = C_3H_7CH(OO^{\bullet})(OOH)$	1.0×10^{19}	−2.5	0	(33)
$CH_2(OOH)C_2H_4C(=O)OCH^{\bullet}{}_2 + O_2 = CH_2(OOH)C_2H_4C(=O)OCH_2(OO^{\bullet})$	1.0×10^{18}	−2.5	0	(34)
$CH_2(OOH)C(=O)OCH^{\bullet}{}_2 + O_2 = CH_2(OOH)C(=O)OCH_2(OO^{\bullet})$	1.0×10^{18}	−2.5	0	(35)
$^{\bullet}CH(OOH)C(=O)OCH_3 + O_2 = CH(OO^{\bullet})(OOH)C(=O)OCH_3$	2.0×10^{18}	−2.5	0	(36)
$C_2H^{\bullet}{}_5C(OOH)C(=O)OCH_3 + O_2 = C_2H_5C(OO^{\bullet})(OOH)C(=O)OCH_3$	1.1×10^{19}	−2.5	0	(37)
$CH^{\bullet}{}_3C(OOH)CH_2C(=O)OCH_3 + O_2 = CH_3C(OO^{\bullet})(OOH)CH_2C(=O)OCH_3$	1.8×10^{19}	−2.5	0	(38)
$^{\bullet}CH(OOH)C_2H_4C(=O)OCH_3 + O_2 = CH(OO^{\bullet})(OOH)C_2H_4C(=O)OCH_3$	1.0×10^{19}	−2.5	0	(39)
$^{\bullet}CH_2C(=O)OCH_2(OOH) + O_2 = CH_2(OO^{\bullet})C(=O)OCH_2(OOH)$	1.0×10^{18}	−2.5	0	(40)
$^{\bullet}CH_2C_2H_4C(=O)OCH_2(OOH) + O_2 = CH_2(OO^{\bullet})C_2H_4C(=O)OCH_2(OOH)$	9.0×10^{18}	−2.5	0	(41)
$C_2H^{\bullet}{}_5CH(OOH) + O_2 = C_2H_5CH(OO^{\bullet})(OOH)$	1.0×10^{19}	−2.5	0	(42)
$CH_3CH(OOH)CH^{\bullet}{}_2 + O_2 = CH_3CH(OOH)CH_2(OO^{\bullet})$	1.5×10^{18}	−2.5	0	(43)
$iC_3H^{\bullet}{}_7 + O_2 = CH_3CH(OO^{\bullet})CH_3$	1.6×10^{19}	−2.5	0	(44)
Isomerizations				
$^{\bullet}CH_2C_2H_4C(=O)OCH_3 = C_3H_7C(=O)OCH^{\bullet}{}_2$	2.5×10^{7}	1.0	17,900	(45)
$C_3H_7C(=O)OCH^{\bullet}{}_2 = C_2H^{\bullet}{}_5CHC(=O)OCH_3$	5.7×10^{8}	1.0	21,300	(46)
$C_3H_7C(=O)OCH^{\bullet}{}_2 = CH^{\bullet}{}_3CHCH_2C(=O)OCH_3$	9.9×10^{7}	1.0	18,000	(47)
$C_3H_7(OO^{\bullet}) = CH^{\bullet}{}_3CHCH_2(OOH)$	3.3×10^{9}	1.0	32,500	(48)
$C_3H_7(OO^{\bullet}) = {}^{\bullet}CH_2C_2H_4(OOH)$	8.6×10^{8}	1.0	28,500	(49)
$C_4H_9(OO^{\bullet}) = C_2H^{\bullet}{}_5CHCH_2(OOH)$	3.3×10^{9}	1.0	32,500	(50)
$C_4H_9(OO^{\bullet}) = CH^{\bullet}{}_3CHC_2H_4(OOH)$	5.7×10^{8}	1.0	25,500	(51)
$C_4H_9(OO^{\bullet}) = {}^{\bullet}CH_2C_3H_6(OOH)$	1.5×10^{8}	1.0	25,000	(52)
$CH2(OO^{\bullet})C_2H_4C(=O)OCH_3 = CH_2(OOH)^{\bullet}CHCH_2C(=O)OCH_3$	3.3×10^{9}	1.0	32,500	(53)
$CH2(OO^{\bullet})C_2H_4C(=O)OCH_3 = CH_2(OOH)CH^{\bullet}{}_2CHC(=O)OCH_3$	5.7×10^{8}	1.0	22,500	(54)
$^{\bullet}CH_2C(=O)OCH_3 = CH_3C(=O)OCH^{\bullet}{}_2$	8.6×10^{8}	1.0	17,800	(55)
$C_3H_7C(=O)OCH_2(OO^{\bullet}) = C_2H^{\bullet}{}_5CHC(=O)OCH_2(OOH)$	9.9×10^{7}	1.0	24,700	(56)
$C_3H_7C(=O)OCH_2(OO^{\bullet}) = CH^{\bullet}{}_3CHCH_2C(=O)OCH_2(OOH)$	1.7×10^{7}	1.0	23,700	(57)
$C_2H_5CH(OO^{\bullet})C(=O)OCH_3 = CH^{\bullet}{}_3CHCH(OOH)C(=O)OCH_3$	3.3×10^{9}	1.0	32,500	(58)
$C_2H_5CH(OO^{\bullet})C(=O)OCH_3 = {}^{\bullet}CH_2CH_2CH(OOH)C(=O)OCH_3$	8.6×10^{8}	1.0	28,500	(59)
$C_2H_5CH(OO^{\bullet})C(=O)OCH_3 = C_2H_5CH(OOH)C(=O)OCH^{\bullet}{}_2$	1.5×10^{8}	1.0	25,700	(60)
$CH_3CH(OO^{\bullet})CH_2C(=O)OCH_3 = {}^{\bullet}CH_2CH(OOH)CH_2C(=O)OCH_3$	5.0×10^{9}	1.0	35,500	(61)
$CH_3CH(OO^{\bullet})CH_2C(=O)OCH_3 = CH_3CH(OOH)^{\bullet}CHC(=O)OCH_3$	3.3×10^{9}	1.0	29,500	(62)
$CH_3CH(OO^{\bullet})CH_2C(=O)OCH_3 = CH_3CH(OOH)CH_2C(=O)OCH^{\bullet}{}_2$	2.5×10^{7}	1.0	24,700	(63)
$^{\bullet}CH_2C_3H_6OOH = C_3H^{\bullet}{}_7CH(OOH)$	5.7×10^{8}	1.0	15,300	(64)
$CH_2(OOH)^{\bullet}CHCH_2C(=O)OCH_3 = CH_2(OOH)C_2H_4C(=O)OCH^{\bullet}{}_2$	1.5×10^{8}	1.0	12,500	(65)
$CH_2(OOH)CH^{\bullet}{}_2CHC(=O)OCH_3 = CH_2(OOH)C_2H_4C(=O)OCH^{\bullet}{}_2$	8.6×10^{8}	1.0	17,800	(66)
$CH_2(OO^{\bullet})C(=O)OCH_3 = CH_2(OOH)C(=O)OCH^{\bullet}{}_2$	1.5×10^{8}	1.0	25,700	(67)
$C_2H^{\bullet}{}_5CHC(=O)OCH_2(OOH) = C_3H_7C(=O)O^{\bullet}CH(OOH)$	5.7×10^{8}	1.0	14,300	(68)
$CH^{\bullet}{}_3CHCH_2C(=O)OCH_2(OOH) = C_3H_7C(=O)O^{\bullet}CH(OOH)$	9.9×10^{7}	1.0	9,000	(69)
$CH^{\bullet}{}_3CHCH(OOH)C(=O)OCH_3 = C_2H_5CH(OOH)C(=O)OCH^{\bullet}{}_2$	1.5×10^{8}	1.0	12,500	(70)
$^{\bullet}CH_2CH_2CH(OOH)C(=O)OCH_3 = C_2H_5CH(OOH)C(=O)OCH^{\bullet}{}_2$	2.5×10^{7}	1.0	17,900	(71)

Reactions	A	n	E_a	Equation Number
$C_2H_5CH(OOH)C(=O)OCH^{\bullet}_2 = C_2H^{\bullet}_5C(OOH)C(=O)OCH_3$	2.9×10^8	1.0	10,300	(72)
$^{\bullet}CH_2CH(OOH)CH_2C(=O)OCH_3 = CH_3CH(OOH)CH_2C(=O)OCH^{\bullet}_2$	2.5×10^7	1.0	17,900	(73)
$CH_3CH(OOH)^{\bullet}CHC(=O)OCH_3 = CH_3CH(OOH)CH_2C(=O)OCH^{\bullet}_2$	8.6×10^8	1.0	17,800	(74)
$CH_3CH(OOH)CH_2C(=O)OCH^{\bullet}_2 = CH^{\bullet}_3C(OOH)CH_2C(=O)OCH_3$	4.9×10^7	1.0	14,000	(75)
$CH_2(OOH)C_2H_4C(=O)OCH^{\bullet}_2 = ^{\bullet}CH(OOH)C_2H_4C(=O)OCH_3$	1.7×10^7	1.0	21,400	(76)
$CH_2(OOH)C(=O)OCH^{\bullet}_2 = ^{\bullet}CH(OOH)C(=O)OCH_3$	5.7×10^8	1.0	19,300	(77)
$CH_3C(=O)OCH_2(OO^{\bullet}) = ^{\bullet}CH_2C(=O)OCH_2(OOH)$	1.5×10^8	1.0	27,700	(78)
$C_3H_7C(=O)O^{\bullet}CH(OOH) = ^{\bullet}CH_2C_2H_4C(=O)OCH_2(OOH)$	2.5×10^7	1.0	26,900	(79)
$CH_2(OOH)C(=O)OCH^{\bullet}_2 = ^{\bullet}CH(OOH)C(=O)OCH_3$	5.7×10^8	1.0	14,300	(80)
$CH_3CH(OO^{\bullet})CH_3 = CH_3CH(OOH)CH^{\bullet}_2$	1.0×10^{10}	1.0	33,500	(81)
Decomposition of OOQOOH radicals into branching agents				
$CH_3CH(OO^{\bullet})CH_2(OOH) \rightarrow {}^{\bullet}OH + C_3H_6O_3KP$	5.0×10^9	1.0	35,500	(82)
$CH_3CH(OO^{\bullet})CH_2(OOH) \rightarrow {}^{\bullet}OH + C_3H_6O_3KP$	3.3×10^9	1.0	30,500	(83)
$CH_2(OO^{\bullet})C_2H_4(OOH) \rightarrow {}^{\bullet}OH + C_3H_6O_3KP$	3.3×10^9	1.0	32,500	(84)
$CH_2(OO^{\bullet})C_2H_4(OOH) \rightarrow {}^{\bullet}OH + C_3H_6O_3KP$	5.7×10^8	1.0	23,500	(85)
$C_2H_5CH(OO^{\bullet})CH_2(OOH) \rightarrow {}^{\bullet}OH + C_4H_8O_3KP$	3.3×10^9	1.0	30,500	(86)
$C_2H_5CH(OO^{\bullet})CH_2(OOH) \rightarrow {}^{\bullet}OH + C_4H_8O_3KP$	3.3×10^9	1.0	32,500	(87)
$C_2H_5CH(OO^{\bullet})CH_2(OOH) \rightarrow {}^{\bullet}OH + C_4H_8O_3KP$	8.6×10^8	1.0	28,500	(88)
$CH_2(OOH)CH_2CH(OO^{\bullet})CH_3 \rightarrow {}^{\bullet}OH + C_4H_8O_3KP$	5.0×10^9	1.0	35,500	(89)
$CH_2(OOH)CH_2CH(OO^{\bullet})CH_3 \rightarrow {}^{\bullet}OH + C_4H_8O_3KP$	3.3×10^9	1.0	32,500	(90)
$CH_2(OOH)CH_2CH(OO^{\bullet})CH_3 \rightarrow {}^{\bullet}OH + C_4H_8O_3KP$	5.7×10^8	1.0	23,500	(91)
$CH_2(OOH)C_3H_6(OO^{\bullet}) \rightarrow {}^{\bullet}OH + C_4H_8O_3KP$	5.7×10^8	1.0	32,500	(92)
$CH_2(OOH)C_3H_6(OO^{\bullet}) \rightarrow {}^{\bullet}OH + C_4H_8O_3KP$	5.7×10^8	1.0	25,500	(93)
$CH_2(OOH)C_3H_6(OO^{\bullet}) \rightarrow {}^{\bullet}OH + C_4H_8O_3KP$	9.9×10^7	1.0	20,000	(94)
$CH_2(OOH)CH(OO^{\bullet})CH_2C(=O)OCH_3 \rightarrow {}^{\bullet}OH + C_5H_8O_5KPS$	3.3×10^9	1.0	30,500	(95)
$CH_2(OOH)CH(OO^{\bullet})CH_2C(=O)OCH_3 \rightarrow {}^{\bullet}OH + C_5H_8O_5KPS$	3.3×10^9	1.0	29,500	(96)
$CH_2(OOH)CH(OO^{\bullet})CH_2C(=O)OCH_3 \rightarrow {}^{\bullet}OH + C_5H_8O_5KPS$	2.5×10^7	1.0	24,700	(97)
$CH_2(OOH)CH_2CH(OO^{\bullet})C(=O)OCH_3 \rightarrow {}^{\bullet}OH + C_5H_8O_5KPS$	3.3×10^9	1.0	32,500	(98)
$CH_2(OOH)CH_2CH(OO^{\bullet})C(=O)OCH_3 \rightarrow {}^{\bullet}OH + C_5H_8O_5KPS$	5.7×10^8	1.0	23,500	(99)
$CH_2(OOH)CH_2CH(OO^{\bullet})C(=O)OCH_3 \rightarrow {}^{\bullet}OH + C_5H_8O_5KPS$	1.5×10^8	1.0	25,700	(100)
$C_2H_5CH(OO^{\bullet})C(=O)OCH_2(OOH) \rightarrow {}^{\bullet}OH + C_5H_8O_5KPS$	3.3×10^9	1.0	32,500	(101)
$C_2H_5CH(OO^{\bullet})C(=O)OCH_2(OOH) \rightarrow {}^{\bullet}OH + C_5H_8O_5KPS$	8.6×10^8	1.0	28,500	(102)
$C_2H_5CH(OO^{\bullet})C(=O)OCH_2(OOH) \rightarrow {}^{\bullet}OH + C_5H_8O_5KPS$	9.9×10^7	1.0	21,700	(103)
$CH_3CH(OO^{\bullet})CH_2C(=O)OCH_2(OOH) \rightarrow {}^{\bullet}OH + C_5H_8O_5KPS$	5.0×10^9	1.0	35,500	(104)
$CH_3CH(OO^{\bullet})CH_2C(=O)OCH_2(OOH) \rightarrow {}^{\bullet}OH + C_5H_8O_5KPS$	3.3×10^9	1.0	29,500	(105)
$CH_3CH(OO^{\bullet})CH_2C(=O)OCH_2(OOH) \rightarrow {}^{\bullet}OH + C_5H_8O_5KPS$	1.7×10^7	1.0	20,700	(106)
$CH_3CH(OO^{\bullet})CH(OOH)C(=O)OCH_3 \rightarrow {}^{\bullet}OH + C_5H_8O_5KPS$	5.0×10^9	1.0	35,500	(107)
$CH_3CH(OO^{\bullet})CH(OOH)C(=O)OCH_3 \rightarrow {}^{\bullet}OH + C_5H_8O_5KPS$	1.7×10^9	1.0	13,500	(108)
$CH_3CH(OO^{\bullet})CH(OOH)C(=O)OCH_3 \rightarrow {}^{\bullet}OH + C_5H_8O_5KPS$	2.5×10^7	1.0	24,700	(109)
$CH_2(OO^{\bullet})CH_2CH(OOH)C(=O)OCH_3 \rightarrow {}^{\bullet}OH + C_5H_8O_5KPS$	3.3×10^9	1.0	32,500	(110)
$CH_2(OO^{\bullet})CH_2CH(OOH)C(=O)OCH_3 \rightarrow {}^{\bullet}OH + C_5H_8O_5KPS$	2.9×10^8	1.0	6,500	(111)
$C_2H_5CH(OOH)C(=O)OCH_2(OO^{\bullet} \rightarrow {}^{\bullet}OH + C_5H_8O_5KPS$	4.9×10^7	1.0	19,700	(112)
$C_2H_5CH(OOH)C(=O)OCH_2(OO^{\bullet} \rightarrow {}^{\bullet}OH + C_5H_8O_5KPS$	1.7×10^7	1.0	23,700	(113)
$CH2(OO^{\bullet})CH(OOH)CH_2C(=O)OCH_3 \rightarrow {}^{\bullet}OH + C_5H_8O_5KPS$	1.7×10^9	1.0	27,500	(114)
$CH_2(OO^{\bullet})CH(OOH)CH_2C(=O)OCH_3 \rightarrow {}^{\bullet}OH + C_5H_8O_5KPS$	5.7×10^8	1.0	22,500	(115)
$CH_3CH(OOH)CH(OO^{\bullet})C(=O)OCH_3 \rightarrow {}^{\bullet}OH + C_5H_8O_5KPS$	1.7×10^9	1.0	27,500	(116)
$CH_3CH(OOH)CH(OO^{\bullet})C(=O)OCH_3 \rightarrow {}^{\bullet}OH + C_5H_8O_5KPS$	8.6×10^8	1.0	28,500	(117)
$CH_3CH(OOH)CH(OO^{\bullet})C(=O)OCH_3 \rightarrow {}^{\bullet}OH + C_5H_8O_5KPS$	1.5×10^8	1.0	25,700	(118)
$CH_3CH(OOH)CH_2C(=O)OCH_2(OO^{\bullet}) \rightarrow {}^{\bullet}OH + C_5H_8O_5KPS$	9.9×10^7	1.0	24,700	(119)
$CH_3CH(OOH)CH_2C(=O)OCH_2(OO^{\bullet}) \rightarrow {}^{\bullet}OH + C_5H_8O_5KPS$	8.5×10^6	1.0	18,700	(120)
$C_3H_7CH(OOH)(OO^{\bullet}) \rightarrow {}^{\bullet}OH + C_4H_8O_3KP$	3.3×10^9	1.0	32,500	(121)
$C_3H_7CH(OOH)(OO^{\bullet}) \rightarrow {}^{\bullet}OH + C_4H_8O_3KP$	5.7×10^8	1.0	25,500	(122)
$C_3H_7CH(OOH)(OO^{\bullet}) \rightarrow {}^{\bullet}OH + C_4H_8O_3KP$	1.5×10^8	1.0	25,000	(123)

Reactions	A	n	E_a	Equation Number
$CH_2(OOH)C_2H_4C(=O)OCH_2(OO^\bullet) \rightarrow {}^\bullet OH + C_5H_8O_5$ *KPS*	9.9×10^7	1.0	24,700	(124)
$CH_2(OOH)C_2H_4C(=O)OCH_2(OO^\bullet) \rightarrow {}^\bullet OH + C_5H_8O_5$ *KPS*	1.7×10^7	1.0	23,700	(125)
$CH_2(OOH)C(=O)OCH2(OO^\bullet \rightarrow {}^\bullet OH + C_3H_4O_5$ *KPS*	9.9×10^7	1.0	22,700	(126)
$CH(OOH)(OO^\bullet)C(=O)OCH_3 \rightarrow {}^\bullet OH + C_3H_4O_5$ *KPS*	1.5×10^8	1.0	25,700	(127)
$C_2H_5C(OOH)(OO^\bullet)C(=O)OCH_3 \rightarrow {}^\bullet OH + C_5H_8O_5$ *KPS*	3.3×10^9	1.0	32,500	(128)
$C_2H_5C(OOH)(OO^\bullet)C(=O)OCH_3 \rightarrow {}^\bullet OH + C_5H_8O_5$ *KPS*	8.6×10^8	1.0	28,500	(129)
$C_2H_5C(OOH)(OO^\bullet)C(=O)OCH_3 \rightarrow {}^\bullet OH + C_5H_8O_5$ *KPS*	1.5×10^8	1.0	25,700	(130)
$CH_3C(OOH)(OO^\bullet)CH_2C(=O)OCH_3 \rightarrow {}^\bullet OH + C_5H_8O_5$ *KPS*	5.0×10^9	1.0	35,500	(131)
$CH_3C(OOH)(OO^\bullet)CH_2C(=O)OCH_3 \rightarrow {}^\bullet OH + C_5H_8O_5$ *KPS*	3.3×10^9	1.0	29,500	(132)
$CH_3C(OOH)(OO^\bullet)CH_2C(=O)OCH_3 \rightarrow {}^\bullet OH + C_5H_8O_5$ *KPS*	2.5×10^7	1.0	24,700	(133)
$CH(OO^\bullet)(OOH)C_2H_4C(=O)OCH_3 \rightarrow {}^\bullet OH + C_5H_8O_5$ *KPS*	3.3×10^9	1.0	32,500	(134)
$CH(OO^\bullet)(OOH)C_2H_4C(=O)OCH_3 \rightarrow {}^\bullet OH + C_5H_8O_5$ *KPS*	5.7×10^8	1.0	22,500	(135)
$CH_2(OO^\bullet)C(=O)OCH_2(OOH) \rightarrow {}^\bullet OH + C_3H_4O_5$ *KPS*	9.9×10^7	1.0	21,700	(136)
$CH_2(OO^\bullet)C_2H_4C(=O)OCH_2(OOH) \rightarrow {}^\bullet OH + C_5H_8O_5$ *KPS*	3.3×10^9	1.0	32,500	(137)
$CH_2(OO^\bullet)C_2H_4C(=O)OCH_2(OOH) \rightarrow {}^\bullet OH + C_5H_8O_5$ *KPS*	5.7×10^8	1.0	22,500	(138)
$C_2H_5CH(OOH)(OO^\bullet) \rightarrow {}^\bullet OH + C_3H_6O_3$ *KP*	3.3×10^9	1.0	32,500	(139)
$C_2H_5CH(OOH)(OO^\bullet) \rightarrow {}^\bullet OH + C_3H_6O_3$ *KP*	8.6×10^8	1.0	28,500	(140)
$CH_3CH(OOH)CH_2(OO^\bullet) \rightarrow {}^\bullet OH + C_3H_6O_3$ *KP*	1.7×10^9	1.0	27,500	(141)
$CH_3CH(OOH)CH_2(OO^\bullet) \rightarrow {}^\bullet OH + C_3H_6O_3$ *KP*	8.6×10^8	1.0	28,500	(142)
β-scissions				
$nC_3H^\bullet_7 \rightarrow {}^\bullet CH_3 + C_2H_4$	2.0×10^{13}	0.0	31,000	(143)
$nC_3H^\bullet_7 \rightarrow {}^\bullet H + C_3H_6$	3.0×10^{13}	0.0	38,000	(144)
$nC_4H^\bullet_9 \rightarrow {}^\bullet C_2H_5 + C_2H_4$	2.0×10^{13}	0.0	27,800	(145)
$nC_4H^\bullet_9 \rightarrow {}^\bullet H + C_4H_8Y$	3.0×10^{13}	0.0	38,000	(146)
${}^\bullet CH_2C_2H_4C(=O)OCH_3 \rightarrow {}^\bullet CH_2C(=O)OCH_3 + C_2H_4$	2.1×10^{13}	0.0	27,800	(147)
${}^\bullet CH_2C_2H_4C(=O)OCH_3 \rightarrow {}^\bullet H + C_5H_8O_2$ *ZS*	3.0×10^{13}	0.0	38,000	(148)
$C_3H_7C(=O)OCH^\bullet_2 \rightarrow C_3H^\bullet_7CO + HCHO$	2.1×10^{13}	0.0	31,900	(149)
$C_2H^\bullet_5CHC(=O)OCH_3 \rightarrow {}^\bullet H + C_5H_8O_2$ *ZS*	3.0×10^{13}	0.0	38,000	(150)
$C_2H^\bullet_5CHC(=O)OCH_3 \rightarrow CH_3O^\bullet + C_4H_6O$ *KZ*	2.1×10^{13}	0.0	49,000	(151)
$C_2H^\bullet_5CHC(=O)OCH_3 \rightarrow {}^\bullet CH_3 + C_4H_6O_2$ *ZS*	2.0×10^{13}	0.0	31,000	(152)
$CH^\bullet_3CHCH_2C(=O)OCH_3 \rightarrow CH_3O^\bullet CO + C_3H_6$	2.1×10^{13}	0.0	31,200	(153)
$CH^\bullet_3CHCH_2C(=O)OCH_3 \rightarrow {}^\bullet H + C_5H_8O_2$ *ZS*	3.0×10^{13}	0.0	34,900	(154)
$CH^\bullet_3CHCH_2C(=O)OCH_3 \rightarrow {}^\bullet H + C_5H_8O_2$ *ZS*	3.0×10^{13}	0.0	39,000	(155)
${}^\bullet CH_2C(=O)OCH_3 \rightarrow CH_3O^\bullet + CH_2CO$ *Z*	2.1×10^{13}	0.0	49,000	(156)
$CH^\bullet_3CHCH_2(OOH) \rightarrow HO^\bullet_2 + C_3H_6$	8.5×10^{12}	0.0	26,000	(157)
$CH^\bullet_3CHCH_2(OOH) \rightarrow {}^\bullet H + C_3H_6O_2$ *PZ*	3.0×10^{13}	0.0	38,000	(158)
$CH^\bullet_3CHCH_2(OOH) \rightarrow {}^\bullet H + C_3H_6O_2$ *PZ*	3.0×10^{13}	0.0	39,000	(159)
${}^\bullet CH_2C_2H_4(OOH) \rightarrow {}^\bullet H + C_3H_6O_2$ *PZ*	3.0×10^{13}	0.0	38,000	(160)
$C_2H^\bullet_5CHCH_2(OOH) \rightarrow HO^\bullet_2 + C_4H_8Y$	8.5×10^{12}	0.0	26,000	(161)
$C_2H^\bullet_5CHCH_2(OOH) \rightarrow {}^\bullet CH_3 + C_3H_6O_2$ *PZ*	2.0×10^{13}	0.0	31,000	(162)
$C_2H^\bullet_5CHCH_2(OOH) \rightarrow {}^\bullet H + C_4H_8O_2$ *PZ*	3.0×10^{13}	0.0	38,000	(163)
$C_2H^\bullet_5CHCH_2(OOH) \rightarrow {}^\bullet H + C_4H_8O_2$ *PZ*	3.0×10^{13}	0.0	38,000	(164)
$CH^\bullet_3CHC_2H_4(OOH) \rightarrow {}^\bullet H + C_4H_8O_2$ *PZ*	3.0×10^{13}	0.0	38,000	(165)
$CH^\bullet_3CHC_2H_4(OOH) \rightarrow {}^\bullet H + C_4H_8O_2$ *PZ*	3.0×10^{13}	0.0	39,000	(166)
${}^\bullet CH_2C_3H_6(OOH) \rightarrow {}^\bullet CH_2CH_2(OOH) + C_2H_4$	2.0×10^{13}	0.0	28,700	(167)
${}^\bullet CH_2C_3H_6(OOH) \rightarrow {}^\bullet H + C_4H_8O_2$ *PZ*	3.0×10^{13}	0.0	38,000	(168)
$CH_2(OOH)^\bullet CHCH_2C(=O)OCH_3 \rightarrow HO^\bullet_2 + C_5H_8O_2$ *ZS*	2.1×10^{13}	0.0	49,000	(169)
$CH_2(OOH)^\bullet CHCH_2C(=O)OCH_3 \rightarrow CH_3O^\bullet CO + C_3H_6O_2$ *PZ*	2.1×10^{13}	0.0	31,200	(170)
$CH_2(OOH)^\bullet CHCH_2C(=O)OCH_3 \rightarrow {}^\bullet H + C_5H_8O_4$ *PZS*	3.0×10^{13}	0.0	34,900	(171)
$CH_2(OOH)^\bullet CHCH_2C(=O)OCH_3 \rightarrow {}^\bullet H + C_5H_8O_4$ *PZS*	3.0×10^{13}	0.0	38,000	(172)
$CH_2(OOH)CH^\bullet_2CHC(=O)OCH_3 \rightarrow {}^\bullet H + C_5H_8O_4$ *PZS*	3.0×10^{13}	0.0	38,000	(173)
$CH_2(OOH)CH^\bullet_2CHC(=O)OCH_3 \rightarrow CH_3O^\bullet + C_4H_6O_3$ *KPZ*	2.1×10^{13}	0.0	49,000	(174)
$CH_3C(=O)OCH^\bullet_2 \rightarrow CH^\bullet_3CO + HCHO$	2.1×10^{13}	0.0	31,900	(175)

Reactions	A	n	E_a	Equation Number
$C_2H^{\bullet}{}_5CHC(=O)OCH_2(OOH) \rightarrow {}^{\bullet}H+C_5H_8O_4PZS$	3.0×10^{13}	0.0	38,000	(176)
$C_2H^{\bullet}{}_5CHC(=O)OCH_2(OOH) \rightarrow {}^{\bullet}CH_3+C_4H_6O_4PZS$	2.0×10^{13}	0.0	31,000	(177)
$CH^{\bullet}{}_3CHCH_2C(=O)OCH_2(OOH) \rightarrow {}^{\bullet}H+C_5H_8O_4PZS$	3.0×10^{13}	0.0	38,000	(178)
$CH^{\bullet}{}_3CHCH_2C(=O)OCH_2(OOH) \rightarrow {}^{\bullet}H+C_5H_8O_4PZS$	3.0×10^{13}	0.0	39,000	(179)
$CH^{\bullet}{}_3CHCH(OOH)C(=O)OCH_3 \rightarrow HO^{\bullet}{}_2+C_5H_8O_2ZS$	2.1×10^{13}	0.0	49,000	(180)
$CH^{\bullet}{}_3CHCH(OOH)C(=O)OCH_3 \rightarrow CH_3O^{\bullet}CO+C_3H_6O_2PZ$	2.1×10^{13}	0.0	31,200	(181)
$CH^{\bullet}{}_3CHCH(OOH)C(=O)OCH_3 \rightarrow {}^{\bullet}H+C_5H_8O_4PZS$	1.5×10^{13}	0.0	34,900	(182)
$CH^{\bullet}{}_3CHCH(OOH)C(=O)OCH_3 \rightarrow {}^{\bullet}H+C_5H_8O_4PZS$	3.0×10^{13}	0.0	39,000	(183)
$^{\bullet}CH_2CH_2CH(OOH)C(=O)OCH_3 \rightarrow {}^{\bullet}CH(OOH)C(=O)OCH_3+C_2H_4$	2.1×10^{13}	0.0	27,800	(184)
$^{\bullet}CH_2CH_2CH(OOH)C(=O)OCH_3 \rightarrow {}^{\bullet}H+C_5H_8O_4PZS$	3.0×10^{13}	0.0	38,000	(185)
$C_2H_5CH(OOH)C(=O)OCH^{\bullet}{}_2 \rightarrow C_2H_5CH(OOH)^{\bullet}CO+HCHO$	2.1×10^{13}	0.0	31,900	(186)
$^{\bullet}CH_2CH(OOH)CH_2C(=O)OCH_3 \rightarrow HO^{\bullet}{}_2+C_5H_8O_2ZS$	2.1×10^{13}	0.0	49,000	(187)
$^{\bullet}CH_2CH(OOH)CH_2C(=O)OCH_3 \rightarrow {}^{\bullet}H+C_5H_8O_4PZS$	1.5×10^{13}	0.0	37,500	(188)
$CH_3CH(OOH)^{\bullet}CHC(=O)OCH_3 \rightarrow HO^{\bullet}{}_2+C_5H_8O_2ZS$	2.1×10^{13}	0.0	49,000	(189)
$CH_3CH(OOH)^{\bullet}CHC(=O)OCH_3 \rightarrow {}^{\bullet}H+C_5H_8O_4PZS$	1.5×10^{13}	0.0	37,500	(190)
$CH_3CH(OOH)^{\bullet}CHC(=O)OCH_3 \rightarrow CH_3O^{\bullet}+C_4H_6O_3KPZ$	2.1×10^{13}	0.0	49,000	(191)
$CH_3CH(OOH)^{\bullet}CHC(=O)OCH_3 \rightarrow {}^{\bullet}CH_3+C_4H_6O_4PZS$	2.0×10^{13}	0.0	31,300	(192)
$CH_3CH(OOH)CH_2C(=O)OCH^{\bullet}{}_2 \rightarrow CH_3CH(OOH)CH^{\bullet}{}_2CO+HCHO$	2.1×10^{13}	0.0	31,900	(193)
$C_3H^{\bullet}{}_7CH(OOH) \rightarrow {}^{\bullet}H+C_4H_8O_2PZ$	3.0×10^{13}	0.0	38,000	(194)
$C_3H^{\bullet}{}_7CH(OOH) \rightarrow {}^{\bullet}OH+C_4H_8OA$	1.0×10^{9}	0.0	7,500	(195)
$CH_2(OOH)C_2H_4C(=O)O^{\bullet}CH_2 \rightarrow CH_2(OOH)C_2H^{\bullet}{}_4CO+HCHO$	2.1×10^{13}	0.0	31,900	(196)
$C_3H_7C(=O)O^{\bullet}CHOOH \rightarrow {}^{\bullet}OH+C_5H_8O_3AS$	2.1×10^{13}	0.0	49,000	(197)
$^{\bullet}CH(OOH)C(=O)OCH_3 \rightarrow {}^{\bullet}OH+C_3H_4O_3AS$	2.1×10^{13}	0.0	49,000	(198)
$C_2H^{\bullet}{}_5C(OOH)C(=O)OCH_3 \rightarrow {}^{\bullet}H+C_5H_8O_4PZS$	3.0×10^{13}	0.0	38,000	(199)
$C_2H^{\bullet}{}_5C(OOH)C(=O)OCH_3 \rightarrow CH_3O^{\bullet}+C_4H_6O_3KPZ$	2.1×10^{13}	0.0	49,000	(200)
$C_2H^{\bullet}{}_5C(OOH)C(=O)OCH_3 \rightarrow {}^{\bullet}CH_3+C_4H_6O_4PZS$	2.0×10^{13}	0.0	31,300	(201)
$C_2H^{\bullet}{}_5C(OOH)C(=O)OCH_3 \rightarrow {}^{\bullet}OH+C_5H_8O_3KS$	2.1×10^{13}	0.0	49,000	(202)
$CH^{\bullet}{}_3C(OOH)CH_2C(=O)OCH_3 \rightarrow {}^{\bullet}H+C_5H_8O_4PZS$	3.0×10^{13}	0.0	34,900	(203)
$CH^{\bullet}{}_3C(OOH)CH_2C(=O)OCH_3 \rightarrow {}^{\bullet}H+C_5H_8O_4PZS$	3.0×10^{13}	0.0	39,000	(204)
$CH^{\bullet}{}_3C(OOH)CH_2C(=O)OCH_3 \rightarrow {}^{\bullet}OH+C_5H_8O_3KS$	2.1×10^{13}	0.0	49,000	(205)
$CH^{\bullet}{}_3C(OOH)CH_2C(=O)OCH_3 \rightarrow CH_3O^{\bullet}CO+C_3H_6O_2PY$	2.1×10^{13}	0.0	31,200	(206)
$^{\bullet}CH(OOH)C_2H_4C(=O)OCH_3 \rightarrow {}^{\bullet}H+C_5H_8O_4PZS$	3.0×10^{13}	0.0	38,000	(207)
$^{\bullet}CH(OOH)C_2H_4C(=O)OCH_3 \rightarrow {}^{\bullet}OH+C_5H_8O_3AS$	2.1×10^{13}	0.0	49,000	(208)
$^{\bullet}CH_2C_2H_4C(=O)OCH_2(OOH) \rightarrow {}^{\bullet}CH_2C(=O)OCH_2(OOH)+C_2H_4$	2.0×10^{13}	0.0	28,700	(209)
$^{\bullet}CH_2C_2H_4C(=O)OCH_2(OOH) \rightarrow {}^{\bullet}H+C_5H_8O_4PZS$	3.0×10^{13}	0.0	38,000	(210)
$CH^{\bullet}{}_3CH(OOH)CH_2 \rightarrow HO^{\bullet}{}_2+C_3H_6$	1.0×10^{9}	0.0	7,500	(211)
$CH^{\bullet}{}_3CH(OOH)CH_2 \rightarrow {}^{\bullet}H+C_3H_6O_2PY$	3.0×10^{13}	0.0	38,000	(212)
$CH_3CH(OOH)CH^{\bullet}{}_2 \rightarrow {}^{\bullet}OH+C_2H_5CHO$	8.5×10^{12}	0.0	26,000	(213)
$CH_3CH(OOH)CH^{\bullet}{}_2 \rightarrow {}^{\bullet}H+C_3H_6O_2PZ$	1.5×10^{13}	0.0	37,500	(214)
$CH_3C(=O)O^{\bullet}CH(OOH) \rightarrow {}^{\bullet}OH+C_3H_4O_3AS$	2.1×10^{13}	0.0	49,000	(215)
$iC_3H_7 \rightarrow {}^{\bullet}H+C_3H_6$	6.0×10^{13}	0.0	39,000	(216)
$^{\bullet}CH_2CH_2C(=O)OCH_3 \rightarrow CH_3O^{\bullet}CO+C_2H_4$	2.1×10^{13}	0.0	31,200	(217)
$^{\bullet}CH_2CH_2C(=O)OCH_3 \rightarrow {}^{\bullet}H+C_4H_6O_2ZS$	3.0×10^{13}	0.0	38,000	(218)
$C_3H_7C(=O)O^{\bullet} \rightarrow nC_3H^{\bullet}{}_7+CO_2$	2.0×10^{13}	0.0	5,100	(219)
$^{\bullet}CH_2C_2H_4(OOH) \rightarrow {}^{\bullet}OH+HCHO+C_2H_4$	2.0×10^{13}	0.0	28,700	(220)
$CH^{\bullet}{}_3CHC_2H_4(OOH) \rightarrow {}^{\bullet}OH+HCHO+C_3H_6$	2.0×10^{13}	0.0	28,700	(221)
$CH_2(OOH)CH^{\bullet}{}_2CHC(=O)OCH_3 \rightarrow {}^{\bullet}OH+HCHO+C_4H_6O_2ZS$	2.0×10^{13}	0.0	30,200	(222)
$^{\bullet}CH_2CH(OOH)CH_2C(=O)OCH_3 \rightarrow {}^{\bullet}OH+{}^{\bullet}CH_2CHO+{}^{\bullet}CH_2C(=O)OCH_3$	2.1×10^{13}	0.0	27,800	(223)
$C_3H^{\bullet}{}_7CH(OOH) \rightarrow {}^{\bullet}OH+{}^{\bullet}CH_2CHO+C_2H^{\bullet}{}_5$	2.0×10^{13}	0.0	28,700	(224)
$^{\bullet}CH(OOH)C_2H_4C(=O)OCH_3 \rightarrow {}^{\bullet}OH+{}^{\bullet}CH_2CHO+{}^{\bullet}CH_2C(=O)OCH_3$	2.1×10^{13}	0.0	27,800	(225)
$CH^{\bullet}{}_3C(OOH)CH_3 \rightarrow {}^{\bullet}OH+{}^{\bullet}CH_2CHO+{}^{\bullet}CH_3$	2.0×10^{13}	0.0	31,000	(226)
$CH_3CH(OOH)CH^{\bullet}{}_2 \rightarrow {}^{\bullet}OH+{}^{\bullet}CH_2CHO+{}^{\bullet}CH_3$	2.0×10^{13}	0.0	31,000	(227)

Decomposition of R$^{\bullet}$CO free radicals

Reactions	A	n	E_a	Equation Number
$C_3H^{\bullet}{}_7CO \rightarrow nC_3H^{\bullet}{}_7 + CO$	2.8×10^{13}	0.0	17,150	(228)
$CH_2(OOH)C_2H^{\bullet}{}_4CO \rightarrow {}^{\bullet}CH_2C_2H_4(OOH)+CO$	2.8×10^{13}	0.0	17,150	(229)
$C_2H_5CH(OOH)^{\bullet}CO \rightarrow C_2H^{\bullet}{}_5CH(OOH)+CO$	2.8×10^{13}	0.0	17,150	(230)
$CH_3CH(OOH)CH^{\bullet}{}_2CO \rightarrow CH_3CH(OOH)^{\bullet}CH_2 + CO$	2.8×10^{13}	0.0	17,150	(231)
Decomposition to o-rings				
$CH^{\bullet}{}_3CHCH_2(OOH) \rightarrow {}^{\bullet}OH+C_3H_6O$*E#3*	6.1×10^{11}	0.0	17,950	(232)
${}^{\bullet}CH_2CH_2CH_2(OOH) \rightarrow {}^{\bullet}OH+C_3H_6O$*E#4*	9.2×10^{10}	0.0	16,600	(233)
$C_2H^{\bullet}{}_5CHCH_2(OOH) \rightarrow {}^{\bullet}OH+C_4H_8O$*E#3*	6.1×10^{11}	0.0	17,950	(234)
$CH^{\bullet}{}_3CHCH_2CH_2(OOH) \rightarrow {}^{\bullet}OH+C_4H_8O$*E#4*	9.2×10^{10}	0.0	16,600	(235)
${}^{\bullet}CH_2C_2H_4CH_2(OOH) \rightarrow {}^{\bullet}OH+C_4H_8O$*E#5*	3.6×10^{9}	0.0	7,000	(236)
$CH_2(OOH)^{\bullet}CHCH_2C(=O)OCH_3 \rightarrow {}^{\bullet}OH+C_5H_8O_3$*E#3S*	6.1×10^{11}	0.0	17,950	(237)
$CH_2(OOH)CH^{\bullet}{}_2CHC(=O)OCH_3 \rightarrow {}^{\bullet}OH+C_5H_8O_3$*E#4S*	9.2×10^{10}	0.0	16,600	(238)
$C_2H^{\bullet}{}_5CHC(=O)OCH_2(OOH) \rightarrow {}^{\bullet}OH+C_5H_8O_3$*E#4S*	9.2×10^{10}	0.0	16,600	(239)
$CH^{\bullet}{}_3CHCH_2C(=O)OCH_2(OOH) \rightarrow {}^{\bullet}OH+C_5H_8O_3$*E#4S*	3.6×10^{9}	0.0	7,000	(240)
$CH^{\bullet}{}_3CHCH(OOH)C(=O)OCH_3 \rightarrow {}^{\bullet}OH+C_5H_8O_3$*E#3S*	6.1×10^{11}	0.0	17,950	(241)
${}^{\bullet}CH_2CH_2CH(OOH)C(=O)OCH_3 \rightarrow {}^{\bullet}OH+C_5H_8O_3$*E#4S*	9.2×10^{10}	0.0	16,600	(242)
$C_2H_5CH(OOH)C(=O)O^{\bullet}CH_2 \rightarrow {}^{\bullet}OH+C_5H_8O_3$*ES#5*	9.2×10^{10}	0.0	16,600	(243)
${}^{\bullet}CH_2CH(OOH)CH_2C(=O)OCH_3 \rightarrow {}^{\bullet}OH+C_5H_8O_3$*E#3S*	6.1×10^{11}	0.0	17,950	(244)
$CH_3CH(OOH)^{\bullet}CHC(=O)OCH_3 \rightarrow {}^{\bullet}OH+C_5H_8O_3$*E#3S*	6.1×10^{11}	0.0	17,950	(245)
$CH_3CH(OOH)CH_2C(=O)O^{\bullet}CH_2 \rightarrow {}^{\bullet}OH+C_5H_8O_3$*ES#6*	3.6×10^{9}	0.0	7,000	(246)
$CH_2(OOH)C(=O)O^{\bullet}CH_2 \rightarrow {}^{\bullet}OH+C_3H_4O_3$*ES#5*	9.2×10^{10}	0.0	16,600	(247)
${}^{\bullet}CH_2C(=O)OCH_2(OOH) \rightarrow {}^{\bullet}OH+C_3H_4O_3$*ES#5*	9.2×10^{10}	0.0	16,600	(248)
$CH_3CH(OOH)^{\bullet}CH_2 \rightarrow {}^{\bullet}OH+C_3H_6O$*E#3*	6.1×10^{11}	0.0	17,950	(249)
Oxidations				
$nC_3H^{\bullet}{}_7 + O_2 \rightarrow C_3H_6 + HO^{\bullet}{}_2$	2.8×10^{12}	0.0	5,000	(250)
$nC_4H^{\bullet}{}_9 + O_2 \rightarrow C_4H_8Y + HO^{\bullet}{}_2$	1.3×10^{12}	0.0	5,000	(251)
${}^{\bullet}CH_2C_2H_4C(=O)OCH_3 + O_2 \rightarrow C_5H_8O_2$*ZS*$+HO^{\bullet}{}_2$	1.9×10^{12}	0.0	5,000	(252)
$C_2H^{\bullet}{}_5CHC(=O)OCH_3 + O_2 \rightarrow C_5H_8O_2$*ZS*$+HO^{\bullet}{}_2$	1.9×10^{12}	0.0	5,000	(253)
$CH^{\bullet}{}_3CHCH_2C(=O)OCH_3 + O_2 \rightarrow C_5H_8O_2$*ZS*$+HO^{\bullet}{}_2$	1.9×10^{12}	0.0	5,000	(254)
$CH^{\bullet}{}_3CHCH_2C(=O)OCH_3 + O_2 \rightarrow C_5H_8O_2$*ZS*$+HO^{\bullet}{}_2$	8.1×10^{11}	0.0	5,000	(255)
$iC_3H^{\bullet}{}_7 + O_2 \rightarrow C_3H_6 + HO^{\bullet}{}_2$	2.3×10^{12}	0.0	5,000	(256)
${}^{\bullet}CH_2CH_2C(=O)OCH_3 + O_2 \rightarrow C_4H_6O_2$*ZS*$+HO^{\bullet}{}_2$	1.3×10^{12}	0.0	5,000	(257)
Metatheses				
$C_5H_{10}O_2S + {}^{\bullet}O^{\bullet} \rightarrow {}^{\bullet}OH + {}^{\bullet}CH_2C_2H_4C(=O)OCH_3$	5.1×10^{13}	0.0	7,850	(258)
$C_5H_{10}O_2S + {}^{\bullet}O^{\bullet} \rightarrow {}^{\bullet}OH+C_3H_7C(=O)OCH^{\bullet}{}_2$	5.1×10^{8}	1.5	4,150	(259)
$C_5H_{10}O_2S + {}^{\bullet}O^{\bullet} \rightarrow {}^{\bullet}OH+C_2H^{\bullet}{}_5CHC(=O)OCH_3$	3.4×10^{8}	1.5	620	(260)
$C_5H_{10}O_2S + {}^{\bullet}O^{\bullet} \rightarrow {}^{\bullet}OH+CH^{\bullet}{}_3CHCH_2C(=O)OCH_3$	2.6×10^{13}	0.0	5,200	(261)
$C_5H_{10}O_2S + {}^{\bullet}H \rightarrow H_2 + {}^{\bullet}CH_2C_2H_4C(=O)OCH_3$	2.9×10^{7}	2.0	7,700	(262)
$C_5H_{10}O_2S + {}^{\bullet}H \rightarrow H_2+C_3H_7C(=O)OCH^{\bullet}{}_2$	7.2×10^{8}	1.5	6,040	(263)
$C_5H_{10}O_2S + {}^{\bullet}H \rightarrow H_2+C_2H^{\bullet}{}_5CHC(=O)OCH_3$	4.8×10^{8}	1.5	2,980	(264)
$C_5H_{10}O_2S + {}^{\bullet}H \rightarrow H_2+CH^{\bullet}{}_3CHCH_2C(=O)OCH_3$	9.0×10^{6}	2.0	5,000	(265)
$C_5H_{10}O_2S + {}^{\bullet}OH \rightarrow H_2O+{}^{\bullet}CH_2C_2H_4C(=O)OCH_3$	2.7×10^{6}	2.0	450	(266)
$C_5H_{10}O_2S + {}^{\bullet}OH \rightarrow H_2O+C_3H_7C(=O)OCH^{\bullet}{}_2$	3.6×10^{6}	2.0	−100	(267)
$C_5H_{10}O_2S + {}^{\bullet}OH \rightarrow H_2O + C_2H^{\bullet}{}_5CHC(=O)OCH_3$	2.4×10^{6}	2.0	−2,450	(268)
$C_5H_{10}O_2S + {}^{\bullet}OH \rightarrow H_2O + CH^{\bullet}{}_3CHCH_2C(=O)OCH_3$	2.6×10^{6}	2.0	−765	(269)
$C_5H_{10}O_2S + HO^{\bullet}{}_2 \rightarrow H_2O_2 + {}^{\bullet}CH_2C_2H_4C(=O)OCH_3$	6.0×10^{11}	0.0	17,000	(270)
$C_5H_{10}O_2S + HO^{\bullet}{}_2 \rightarrow H_2O_2 + C_3H_7C(=O)OCH^{\bullet}{}_2$	4.2×10^{4}	2.7	17,820	(271)
$C_5H_{10}O_2S + HO^{\bullet}{}_2 \rightarrow H_2O_2 + C_2H^{\bullet}{}_5CHC(=O)OCH_3$	2.8×10^{4}	2.7	15,000	(272)
$C_5H_{10}O_2S + HO^{\bullet}{}_2 \rightarrow H_2O_2 + CH^{\bullet}{}_3CHCH_2C(=O)OCH_3$	4.0×10^{11}	0.0	15,500	(273)
$C_5H_{10}O_2S + {}^{\bullet}CH_3 \rightarrow CH_4 + {}^{\bullet}CH_2C_2H_4C(=O)OCH_3$	3.0×10^{-1}	4.0	8,200	(274)
$C_5H_{10}O_2S + {}^{\bullet}CH_3 \rightarrow CH4+C_3H_7C(=O)OCH^{\bullet}{}_2$	2.4×10^{6}	1.9	9,570	(275)
$C_5H_{10}O_2S + {}^{\bullet}CH_3 \rightarrow CH_4 + C_2H^{\bullet}{}_5CHC(=O)OCH_3$	1.6×10^{6}	1.9	6,510	(276)
$C_5H_{10}O_2S + {}^{\bullet}CH_3 \rightarrow CH_4 + CH^{\bullet}{}_3CHCH_2C(=O)OCH_3$	2.0×10^{11}	0.0	9,600	(277)

Reactions	A	n	E_a	Equation Number
$C_5H_{10}O_2S + {}^{\bullet}CHO \rightarrow HCHO + {}^{\bullet}CH_2C_2H_4C(=O)OCH_3$	1.0×10^5	2.5	18,500	(278)
$C_5H_{10}O_2S + {}^{\bullet}CHO \rightarrow HCHO + C_3H_7C(=O)OCH^{\bullet}{}_2$	1.6×10^7	1.9	17,000	(279)
$C_5H_{10}O_2S + {}^{\bullet}CHO \rightarrow HCHO + C_2H^{\bullet}{}_5CHC(=O)OCH_3$	6.8×10^4	2.5	13,500	(280)
$C_5H_{10}O_2S + {}^{\bullet}CHO \rightarrow HCHO+CH^{\bullet}{}_3CHCH_2C(=O)OCH_3$	1.0×10^7	1.9	17,000	(281)
$C_5H_{10}O_2S + {}^{\bullet}CH_2OH \rightarrow CH_3OH + {}^{\bullet}CH_2C_2H_4C(=O)OCH_3$	9.9×10^1	3.0	14,000	(282)
$C_5H_{10}O_2S + {}^{\bullet}CH_2OH \rightarrow CH_3OH+C_3H_7C(=O)OCH^{\bullet}{}_2$	9.0×10^1	3.0	12,000	(283)
$C_5H_{10}O_2S + {}^{\bullet}CH_2OH \rightarrow CH_3OH+C_2H^{\bullet}{}_5CHC(=O)OCH_3$	2.4×10^2	2.8	10,800	(284)
$C_5H_{10}O_2S + {}^{\bullet}CH_2OH \rightarrow CH3OH+CH_3CHCH_2C(=O)OCH_3$	6.0×10^1	3.0	12,000	(285)
$C_5H_{10}O_2S + CH_3O^{\bullet} \rightarrow CH_3OH+CH_2C_2H_4C(=O)OCH_3$	1.6×10^{11}	0.0	7,300	(286)
$C_5H_{10}O_2S + CH_3O^{\bullet} \rightarrow CH_3OH+C_3H_7C(=O)OCH^{\bullet}{}_2$	2.2×10^{11}	0.0	4,500	(287)
$C_5H_{10}O_2S + CH_3O^{\bullet} \rightarrow CH_3OH+C_2H^{\bullet}{}_5CHC(=O)OCH_3$	4.6×10^{10}	0.0	2,900	(288)
$C_5H_{10}O_2S + CH_3O^{\bullet} \rightarrow CH_3OH+CH^{\bullet}{}_3CHCH_2C(=O)OCH_3$	1.5×10^{11}	0.0	4,500	(289)
$C_5H_{10}O_2S + CH_3OO^{\bullet} \rightarrow CH_3OOH + {}^{\bullet}CH_2C_2H_4C(=O)OCH_3$	6.0×10^{12}	0.0	20,000	(290)
$C_5H_{10}O_2S + CH_3OO^{\bullet} \rightarrow CH_3OOH+C_3H_7C(=O)OCH^{\bullet}{}_2$	4.5×10^{12}	0.0	17,500	(291)
$C_5H_{10}O_2S + CH_3OO^{\bullet} \rightarrow CH_3OOH+C_2H^{\bullet}{}_5CHC(=O)OCH_3$	3.0×10^{12}	0.0	15,000	(292)
$C_5H_{10}O_2S + CH_3OO^{\bullet} \rightarrow CH_3OOH+CH^{\bullet}{}_3CHCH_2C(=O)OCH_3$	3.0×10^{12}	0.0	17,500	(293)
$C_5H_{10}O_2S + C_2H^{\bullet}{}_5 \rightarrow C_2H_6 + {}^{\bullet}CH_2C_2H_4C(=O)OCH_3$	3.0×10^{11}	0.0	13,500	(294)
$C_5H_{10}O_2S + C_2H^{\bullet}{}_5 \rightarrow C_2H_6 +C_3H_7C(=O)OCH^{\bullet}{}_2$	3.0×10^{11}	0.0	11,000	(295)
$C_5H_{10}O_2S + C_2H^{\bullet}{}_5 \rightarrow C_2H_6 + C_2H^{\bullet}{}_5CHC(=O)OCH_3$	2.0×10^{11}	0.0	9,200	(296)
$C_5H_{10}O_2S + C_2H^{\bullet}{}_5 \rightarrow C_2H_6 + CH^{\bullet}{}_3CHCH_2C(=O)OCH_3$	2.0×10^{11}	0.0	11,000	(297)
$C_5H_{10}O_2S + CH_2(OO^{\bullet})C_2H_4C(=O)OCH_3 \rightarrow C_5H_{10}O_4PS+{}^{\bullet}CH_2C_2H_4C(=O)OCH_3$	6.0×10^{12}	0.0	20,000	(298)
$C_5H_{10}O_2S + CH_2(OO^{\bullet})C_2H_4C(=O)OCH_3 \rightarrow C_5H_{10}O_4PS+C_3H_7C(=O)OCH^{\bullet}{}_2$	4.5×10^{12}	0.0	17,500	(299)
$C_5H_{10}O_2S + CH_2(OO^{\bullet})C_2H_4C(=O)OCH_3 \rightarrow C5H10O4PS+C_2H^{\bullet}{}_5CHC(=O)OCH_3$	3.0×10^{12}	0.0	15,000	(300)
$C_5H_{10}O_2S + CH_2(OO^{\bullet})C_2H_4C(=O)OCH_3 \rightarrow C_5H_{10}O_4PS+CH^{\bullet}{}_3CHCH_2C(=O)OCH_3$	3.0×10^{12}	0.0	17,500	(301)
$C_5H_{10}O_2S +C_3H_7C(=O)OCH_2(OO^{\bullet}) \rightarrow C_5H_{10}O_4PS + {}^{\bullet}CH_2C_2H_4C(=O)OCH_3$	6.0×10^{12}	0.0	20,000	(302)
$C_5H_{10}O_2S + C_3H_7C(=O)OCH_2(OO^{\bullet}) \rightarrow C_5H_{10}O_4PS+C_3H_7C(=O)OCH^{\bullet}{}_2$	4.5×10^{12}	0.0	17,500	(303)
$C_5H_{10}O_2S + C_3H_7C(=O)OCH_2(OO^{\bullet}) \rightarrow C_5H_{10}O_4PS+C_2H^{\bullet}{}_5CHC(=O)OCH_3$	3.0×10^{12}	0.0	15,000	(304)
$C_5H_{10}O_2S + C_3H_7C(=O)OCH_2(OO^{\bullet}) \rightarrow C_5H_{10}O_4PS+CH^{\bullet}{}_3CHCH_2C(=O)OCH_3$	3.0×10^{12}	0.0	17,500	(305)
$C_5H_{10}O_2S + C_2H_5CH(OO^{\bullet})C(=O)OCH_3 \rightarrow C_5H_{10}O_4PS + {}^{\bullet}CH_2C_2H_4C(=O)OCH_3$	6.0×10^{12}	0.0	20,000	(306)
$C_5H_{10}O_2S + C_2H_5CH(OO^{\bullet})C(=O)OCH_3 \rightarrow C_5H_{10}O_4PS+C_3H_7C(=O)OCH^{\bullet}{}_2$	4.5×10^{12}	0.0	17,500	(307)
$C_5H_{10}O_2S + C_2H_5CH(OO^{\bullet})C(=O)OCH_3 \rightarrow C_5H_{10}O_4PS+C_2H^{\bullet}{}_5CHC(=O)OCH_3$	3.0×10^{12}	0.0	15,000	(308)
$C_5H_{10}O_2S + C_2H_5CH(OO^{\bullet})C(=O)OCH_3 \rightarrow C_5H_{10}O_4PS+CH^{\bullet}{}_3CHCH_2C(=O)OCH_3$	3.0×10^{12}	0.0	17,500	(309)
$C_5H_{10}O_2S + CH_3CH(OO^{\bullet})CH_2C(=O)OCH_3 \rightarrow C_5H_{10}O_4PS + {}^{\bullet}CH_2C_2H_4C(=O)OCH_3$	6.0×10^{12}	0.0	20,000	(310)
$C_5H_{10}O_2S + CH_3CH(OO^{\bullet})CH_2C(=O)OCH_3 \rightarrow C_5H_{10}O_4PS+C_3H_7C(=O)OCH^{\bullet}{}_2$	4.5×10^{12}	0.0	17,500	(311)
$C_5H_{10}O_2S + CH_3CH(OO^{\bullet})CH_2C(=O)OCH_3 \rightarrow C_5H_{10}O_4PS+C_2H^{\bullet}{}_5CHC(=O)OCH_3$	3.0×10^{12}	0.0	15,000	(312)
$C_5H_{10}O_2S + CH_3CH(OO^{\bullet})CH_2C(=O)OCH_3 \rightarrow C_5H_{10}O_4PS+CH^{\bullet}{}_3CHCH_2C(=O)OCH_3$	3.0×10^{12}	0.0	17,500	(313)
$C_5H_{10}O_2S+iC_3H^{\bullet}{}_7 \rightarrow C_3H_8 + {}^{\bullet}CH_2C_2H_4C(=O)OCH_3$	4.2×10^{-3}	4.2	8,700	(314)
$C_5H_{10}O_2S+iC_3H^{\bullet}{}_7 \rightarrow C_3H_8 + C_3H_7C(=O)OCH^{\bullet}{}_2$	4.2×10^{-3}	4.2	8,000	(315)
$C_5H_{10}O_2S+iC_3H^{\bullet}{}_7 \rightarrow C_3H_8 + C_2H^{\bullet}{}_5CHC(=O)OCH_3$	2.8×10^{-3}	4.2	6,000	(316)
$C_5H_{10}O_2S+iC_3H^{\bullet}{}_7 \rightarrow C3H8+CH^{\bullet}{}_3CHCH_2C(=O)OCH_3$	2.8×10^{-3}	4.2	8,000	(317)
Combinations				
${}^{\bullet}H+iC_3H^{\bullet}{}_7 \rightarrow C_3H_8$	8.3×10^{12}	0.0	0	(318)
${}^{\bullet}OH+iC_3H^{\bullet}{}_7 \rightarrow C_3H_7OH$	5.9×10^{12}	0.0	0	(319)
$HO^{\bullet}{}_2+iC_3H^{\bullet}{}_7 \rightarrow C_3H_8O_2P$	4.8×10^{12}	0.0	0	(320)
$CH^{\bullet}{}_3+iC_3H^{\bullet}{}_7 \rightarrow C_4H_{10}$	1.5×10^{13}	0.0	0	(321)
${}^{\bullet}CHO+iC_3H^{\bullet}{}_7 \rightarrow C_4H_8OA$	5.2×10^{12}	0.0	0	(322)
${}^{\bullet}CH_2OH+iC_3H^{\bullet}{}_7 \rightarrow C_4H_{10}OL$	5.1×10^{12}	0.0	0	(323)
$C_2H^{\bullet}{}_5 + iC_3H^{\bullet}{}_7 \rightarrow C_5H_{12}$	5.2×10^{12}	0.0	0	(324)
$iC_3H^{\bullet}{}_7 + iC_3H^{\bullet}{}_7 \rightarrow C_6H_{14}$	2.3×10^{12}	0.0	0	(325)
Disproportionations				
$C_3H_7(OO^{\bullet})+HO^{\bullet}{}_2 \rightarrow C_3H_8O_2P +O_2$	2.0×10^{11}	0	−1,300	(326)
$C_4H_9(OO^{\bullet})+HO^{\bullet}{}_2 \rightarrow C_4H_{10}O_2P + O_2$	2.0×10^{11}	0	−1,300	(327)
$CH_2(OO^{\bullet})C_2H_4C(=O)OCH_3 + HO^{\bullet}{}_2 \rightarrow C5H10O4PS+O_2$	2.0×10^{11}	0	−1,300	(328)

Reactions	*A*	*n*	E_a	Equation Number
$C_3H_7C(=O)OCH_2(OO^\bullet)+HO^\bullet_2 \rightarrow C_5H_{10}O_4PS+O_2$	2.0×10^{11}	0	−1,300	(329)
$C_2H_5CH(OO^\bullet)C(=O)OCH_3 + HO^\bullet_2 \rightarrow C_5H_{10}O_4PS+O_2$	2.0×10^{11}	0	−1,300	(330)
$CH_3CH(OO^\bullet)CH_2C(=O)OCH_3 + HO^\bullet_2 \rightarrow C_5H_{10}O_4PS+O_2$	2.0×10^{11}	0	−1,300	(331)
$CH_2(OO^\bullet)C(=O)OCH_3 +HO^\bullet_2 \rightarrow C_3H_6O_4PS+O_2$	2.0×10^{11}	0	−1,300	(332)
$CH_3C(=O)OCH_2(OO^\bullet)+HO^\bullet_2 \rightarrow C_3H_6O_4PS+O_2$	2.0×10^{11}	0	−1,300	(333)
$CH_3CH(OO^\bullet)CH_3 + HO^\bullet_2 \rightarrow$ C3H8O2*P*+O_2	2.0×10^{11}	0	−1,300	(334)

[a]The rate constants are given at 1 atm ($k = AT^n \exp(-E_a/RT)$) in cm^3. mol. s. cal units.
[b]*Notes:* For molecules, the letters in italics indicate the chemical functions carried by the molecule.
[c]*A* aldehyde function (-CH=O)
[d]*E* ether function (-O-)
[e]*K* ketone function (-C(=O)-)
[f]*L* alcohol function (-O-H)
[g]*P* hydroperoxide function (-O-O-H)
[h]*S* ester function (-CO-O-CH_3)
[i]*U* peroxy function (-O-O-)
[j]*Z* unsaturation (C=C)
[k]*#x* cyclic molecule with a cycle containing *x* atoms
[l]Owing to the lumping of the products, several reactions are written in duplicate with different rate parameters as they correspond to distinct channels.

For studies at temperature below 1000 K, it is necessary to also consider low-temperature reactions:

- additions of alkyl and hydroperoxyalkyl (•QOOH) radicals to an oxygen molecule,
- isomerizations of alkylperoxy and hydroperoxyalkylperoxy radicals (ROO• and •OOQOOH) involving a cyclic transition state and the transfer of an H-atom,
- decompositions of hydroperoxyalkyl and dihydroperoxyalkyl •$U(OOH)_2$ radicals to form cyclic ethers and •OH radicals, and
- disproportionations of alkylperoxy radicals with •HO_2 to produce hydroperoxides and O_2.
- a lumped secondary mechanism, containing reactions consuming the molecular products of the primary mechanism that do not react in the reaction bases. To have a manageable size, the lumped secondary mechanisms (26) involved lumped reactants: the molecules formed in the primary mechanism, with the same molecular formula and the same functional groups, are lumped into one unique species without distinction between the different isomers. The rules used for writing the reactions of hydroperoxides, aldehydes, ketones, alkenes, and cyclic ethers bearing an ester function have been derived from those recently proposed for alkanes by Biet et al. (23). The writing of the secondary reaction is made to promote the formation of C_{2+} alkyl radicals, the reactions of which are already included in the primary mechanism.
- A C_0–C_2 reaction base, including all the reactions involving radicals or molecules, contains less than three carbon atoms (30), which is periodically updated. As this part of the mechanism concerns small species, pressure-dependent rate constants follow the formalism proposed by Troe (31) and efficiency coefficients have been included, which is not the case in the primary and secondary mechanisms.

Thermochemical data for molecules or radicals are automatically computed using software THERGAS (32) based on group additivity (33), and stored as 14 polynomial coefficients, according to the CHEMKIN II formalism (34). The only change made in the case of esters, was that the bond

dissociation energy of the C-H bonds carried by the atom of carbon just neighboring the ester function has been taken equal to 95.6 kcal/mol as the value proposed by Luo (35) for ethyl propanoate.

The kinetic data of isomerizations, combinations, and the unimolecular decompositions are calculated using software KINGAS (26), based on the thermochemical kinetics methods (33) using the transition state theory or the modified collision theory. The kinetic data, for which the calculation is not possible by KINGAS, are estimated from correlations, which are based on quantitative structure–reactivity relationships and obtained from a literature review (26–29) or are estimated from quantum calculations.

The Primary Mechanism of the Oxidation of Methyl Butanoate

Since no mechanism generated by EXGAS in the case of the oxidation of esters has been yet published, Table IV presents the primary mechanism for the oxidation of methyl butanoate, which contains 334 reactions of this ester or of the produced free radicals. This detailed kinetic model was build in a comprehensive way and contains all reactions pertinent at both low and high temperatures, although experimental data from the literature (12,36) gave no evidence of low-temperature phenomena such as cool flame or negative temperature coefficient for methyl esters smaller than methyl pentanoate.

The stable molecules obtained by decompositions by β-scission, decomposition to give cyclic ethers, oxidations, and terminations are lumped. For instance, the two isomers of methyl crotonate are not distinguished and both written $C_5H_8O_2ZS$. For the additions to oxygen molecules (reactions (10)–(44) in Table IV), the combinations (reactions (318)–(325)) and the disproportionations (reactions (326)–(334)), the kinetic data have directly been derived from those proposed for alkanes and alkyl radicals by Buda et al. 29. For the other types of reactions, the following changes have been considered:

- ✓ *Initiations by Breaking a C-C or a C-O Bond (Reactions (1)–(5))*

In the case of esters, the initiations by breaking of a C[BOND]O bond need also to be taken into account (reactions (4) and (5)) in addition to those by breaking of a C-C bond (reactions (1)–(3)). The activation energy of reaction (3), which involves the breaking of the C-C bond located in α-position from the ester function, has been taken equal to 93 kcal/mol according to the value recently calculated by El-Nahas et al. (37). For the other reactions, the values proposed by El-Nahas et al. (37) and those calculated using KINGAS (26) were in agreement to about ± 2 kcal/mol.

- ✓ *Bimolecular Initiations (Reactions (6)–(9)), Oxidations (Reactions (250)–(257)), and Metatheses (Reactions (258)–(317))*

Bimolecular initiations and metatheses involve an H-abstraction from the initial reactant by oxygen molecules or small radicals, respectively. The small radicals taken into account in metatheses were •O• and •H atoms and •OH, $•HO_2$, $•CH_3$, •CHO, $•CH_2OH$, $•CH_3O$, $•CH_3O_2$, $•C_2H_5$, $•iC_3H_7$, and the four peroxy radicals deriving from the first addition to oxygen. The oxidation of an alkyl radical deriving from a saturated ester leads to $•HO_2$ radicals and to the conjugated unsaturated esters. The

correlations used for bimolecular initiations and oxidations are the same as for alkanes (29). For the abstraction of an H-atom from a carbon atom located in α-position of the ester function (the fastest of the H-abstraction reactions for this type of molecules), the correlations were taken the same as those used for the abstraction of a tertiary H-atom from alkanes, except in the case of the abstractions by •O• and •H atoms and by •OH, $•HO_2$, and $•CH_3$ radicals (reactions 260, 264, 268, 272, and 276). In this case, the rate parameters have been evaluated using an Evans–Polanyi-type correlation from Dean and Bozzelli (38), developed for the abstraction of H-atoms from hydrocarbons:

$$k = n_H A T^n \exp(-\{E_0 - f(\Delta H_0 - \Delta H)\}/RT)$$

where n_H is the number of abstractable H-atoms; A, n, and E_0 are the rate parameters for the case of a metathesis by the considered radical from ethane; ΔH_0 is the enthalpy of the metathesis by the considered radical from ethane; ΔH is the enthalpy of the metathesis by the considered radical from the reacting molecule; f is a correlation factor, the values of which were given by Dean and Bozzelli (38) for each considered radical. For the abstraction of an H-atom from a carbon atom neighboring the O-atom, the correlations were taken the same as those used for the abstraction of a primary H-atom from alkanes, except in the case of the abstractions by •O• and •H atoms and by •OH, $•HO_2$ and $•CH_3$ radicals (reactions 259, 263, 267, 271, and 275). In this case, the rate parameters have also been evaluated using the Evans–Polanyi-type correlation from Dean and Bozzelli (38).

- ✓ *Radical Intramolecular Isomerizations (Reactions (45)–(81)) and Decompositions of •OOQOOH Radicals into Branching Agents (Reactions (82)–(142))*

According to Glaude et al. (39), the isomerization of each •OOQOOH radical and the decomposition of the obtained radicals to give hydroperoxide species are globalized into a single step. As in our previous work (26), the activation energy is set equal to the sum of the activation energy for H-abstraction from the substrate by analogous radicals and the strain energy of the cyclic transition state. The activation energy for abstracting an H-atom from the atom of carbon located in α-position from the ester function has been taken equal to that for the abstraction of a tertiary H-atom in an alkyl radical. The strain energy of the cyclic transition state including seven members among which three oxygen atoms has been increased of about 3 kcal/mol compared to that with only two oxygen atoms.

- ✓ *Decompositions of Radicals by β-Scission (Reactions (143)–(227)) and Decompositions of R•CO Radicals (Reactions (228)–(231))*

The presence of oxygen atoms in the involved radicals can have a significant impact on the values of the activation energies of the decomposition by β-scission. Quantum calculations were performed for model reactions at the CBS-QB3 level of theory using Gaussian03 (40) to estimate these data with a given accuracy of ± 1 kcal/mol. Intrinsic reaction coordinate (IRC) calculations have been systematically performed at the B3LYP 6-31G(d) level of theory on transition states, to ensure that they are correctly connected to the desired reactants and products. Table V displays the values that have been used for the activation energies of the decompositions of oxygenated radicals by

β-scission. The kinetic data for the decompositions of R•CO radicals have been taken equal to the values proposed by Baulch et al. (41) for the decomposition of CH•$_3$CO radicals.

Table V. Activation Energies (kcal/mol) Used for the Decompositions by β-Scission of Oxygenated Radicals Involved in the Oxidation of Methyl and Ethyl Esters.

Types of Reaction	E_a
R/C(//O)/O$^\bullet$ → R$^\bullet$ + CO$_2$[a]	5.1
R/C(//O)/O/CH$^\bullet_2$ → R/C$^\bullet$//O + CH$_2$//O [a]	31.9
R/CH$^\bullet$/C(//O)/O/CH$_3$ → R/CH//C//O + CH$_3$O$^\bullet$[b,c]	49.0
R/CH$^\bullet$/CH$_2$/C(//O)/O/CH$_3$ → R/CH//CH$_2$ + CH$_3$O/C$^\bullet$//O[b,c]	30.7
R/CH$_2$/C$^\bullet$//O → R$^\bullet$ + CH$_2$//C//O[d]	39.9
R/CH$^\bullet$/CH$_2$/C(//O)/O/CH$_3$ → H$^\bullet$ + R/CH//CH/C(//O)/O/CH$_3$[b,c]	34.9
R/C(//O)/O/CH$_2$/CH$^\bullet_2$ → R/C(//O)/O$^\bullet$ + C$_2$H$_4$ [a]	25.1

[a] The calculation was performed for R$^\bullet$ = CH$^\bullet_3$.
[b,c]The calculation was performed for R$^\bullet$ = H$^\bullet$.
[c]The same value is used in the case of ethyl esters.
[d]The calculation was performed for R$^\bullet$ = C$_2$H$^\bullet_5$.

- ✓ *Formation of Cyclic Ethers (Reactions (232)–(249))*

The different obtained cyclic ethers are lumped according to the size of the included ring. As illustrated by Figure 8, two types of ethers can be obtained according to the presence or not of the ester function inside the ring. However the kinetic data have directly been derived from those proposed by Buda et al. (29) for the formation of cyclic ethers in the mechanism of the oxidation of alkanes.

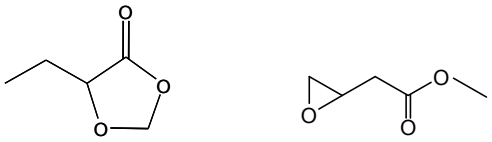

$C_5H_8O_3ES\#5$ $C_5H_8O_3E\#3S$

Figure 8. Examples of cyclic ethers that can be obtained from methyl butanoate.

The Mechanism of the Oxidation of Ethyl Butanoate

The primary and secondary mechanisms for the oxidation of ethyl butanoate have been generated using rules very similar to those described in the case of methyl butanoate. However, since this mechanism can only be validated by modeling shock tube data, only high-temperature reactions have been considered. The activation energies used for the decompositions by β-scission of oxygenated radicals have also been taken from Table V.

The only significant differences with the mechanism of methyl butanoate is the inclusion of the molecular elimination leading to the formation of ethylene and butanoic acid from ethyl butanoate and of the secondary reactions of butanoic acid, for which new rules of generation have to be considered.

This molecular elimination is favored since it occurs through a transition state including a six-membered ring as shown in Figure 9. Molecular eliminations from methyl esters and other channels from ethyl esters can also be envisaged, but theoretical calculations by El-Nahas et al. (37) have shown them to be negligible due to higher energy barriers. The most investigated reaction between the molecular eliminations from ethyl esters giving ethylene and organic acids is that involving ethyl acetate. First kinetic measurements about this reaction in a flow system (42) have led to a A-factor of 3.2×10^{12} s^{-1} with an activation energy of 47.8 kcal/mol. These values are in good agreement with more recent ones measured in a shock tube (43) (A = 10^{12} s^{-1} and Ea = 47.7 kcal/mol) and with the A-factor estimated by Benson (33) (A = 6.2×10^{12} $s^{-}1$ at 700 K). Fewer values have been proposed for heavier ethyl esters. Barnard et al. 44 have measured for ethyl propanoate an A-factor of 5×10^{12} s^{-1} with an activation energy of 48.5 kcal/mol, whereas the calculations of El-Nahas et al. (37) led to an activation energy of 50 kcal/mol. Finally, Kairaitis and Stimson (45) have measured for ethyl butanoate a A-factor of 2×10^{12} s^{-1} with an activation energy of 47.3 kcal/mol, which are the values that we have used in the present mechanism since they are in agreement with the average rate parameters for this type of reaction.

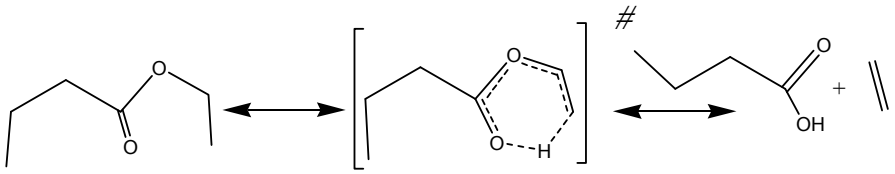

Figure 9. Molecular elimination from ethyl butanoate.

As it will be shown further in the text, the formation of butanoic acid is the main channel consuming ethyl butanoate under the conditions of our shock tube study. To be more accurate for modeling its reactivity, the secondary reactions of this oxygenated species have been generated as if it was an initial reactant: i.e., a comprehensive primary mechanism and a globalized secondary one have been written. The rules of generation of the primary mechanism for the high-temperature oxidation of carboxylic acids are the same as in the case of esters. Only the rate constants used for the abstraction of the H-atom linked to an O-atom by bimolecular oxidation and metatheses have been taken equal to those proposed for a tertiary alkylic H-atom (29). The unimolecular initiation involving the breaking of the O–H bond has been taken into account. The primary reactions of butanoic acid lead to the formation of unsaturated acids, butenoic acids, globalized into one single species ($C_4H_6O_2$ZB), which can react by H-abstractions with small radicals R• (•H, •OH, •HO_2, •CH_3, •CH_3OO, and •C_2H_5) to give RH, CO_2, and allyl radicals.

Comparison between Experimental and Computed Results

Simulations were performed using SENKIN and PSR softwares of CHEMKIN II (34) using the mechanisms previously described, which are available as supplementary material. The mechanism for the oxidation of methyl butanoate ($C_5H_{10}O_2$S-1) involves 203 species and globally contains 1317 reactions (462 reactions are in the reactions bases, 334 in the primary mechanism and 521 in the secondary mechanism). That for the oxidation of ethyl butanoate ($C_6H_{12}O_2$S-1) and butanoic acid ($C_4H_8O_2$B-1) involves 115 species and globally includes 1011 reactions (171 reactions in the primary

mechanism and 378 in the secondary mechanism). While two organic reactants have been considered, the number of reactions in this second mechanism is smaller because only high-temperature reactions are considered.

Simulated ignition delay times have been taken as the time at 10% of the maximum concentration of excited OH* radicals using the mechanism for excited species developed by Hall et al. (46).

- ✓ ***Autoignition and Oxidation of Methyl Butanoate***

Figure 2 shows that the agreement between experimental and simulated ignition delay times of methyl butanoate is satisfactory. Figure 10 shows that our model can also correctly predict the experimental results previously obtained both by Metcalfe et al. (10) and by Walton et al. (13) (within a factor less than 2).

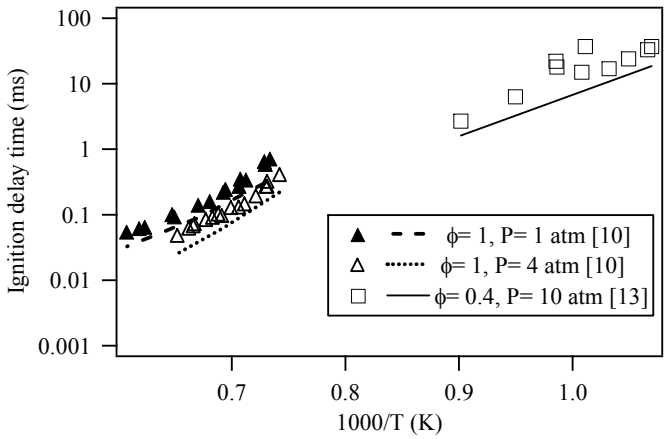

Figure 10. Comparison of model predictions (lines) using the present model with the experimental results (points) of Metcalfe et al. (10) for stoichiometric mixtures at 1 and 4 bar and of Walton et al. (13) for an equivalence ratio of 0.4 at 10 bar.

Figures 5–7 present a comparison between our experimental results and simulations in the case of the oxidation of methyl butanoate in a jet-stirred reactor. While the consumption of oxygen is well reproduced, that of methyl butanoate is overestimated. The formation of methyl acrylate, methyl crotonate, and methane is for the most part correctly modeled, but the agreement deteriorates for other products. While the production of carbon oxides is considerably overestimated in most cases, that of ethylene is underestimated.

Figure 11 presents a comparison between our experimental data at 850 K and modeling results computed using the present model but also those of Fischer et al. (7), Gaïl et al. (9), and Dooley et al. (12). Models developed by Fischer et al. (7) and by Gaïl et al. (9) contain both low- and high-temperature reactions, whereas Dooley et al. (12) considered only high-temperature reactions and the reactions of methyl butanoate alkyl radicals with O_2 and RO_2 radicals. All the four models sensibly overestimate the consumption of methyl butanoate (Figure 3a), especially for the short residence times, and underestimate the production of ethylene (Figure 3c). The underestimation of ethylene is of a factor up to 8 for the models of Fisher et al. (7) and Gaïl et al. (9), while it is only up to 3 for the present model and that of Dooley et al. 12. The production of carbon oxides (Figure 3b) and

methane (Figure 3c) are captured by the four models within a factor better than 1.5. The present model and that of Dooley et al. (12) reproduces the best the time profile of methyl acrylate (Figure 3a), which is overestimated by a factor above 2 for the two other models. That is certainly due to the fact that the more recent models better consider the reactions of unsaturated esters.

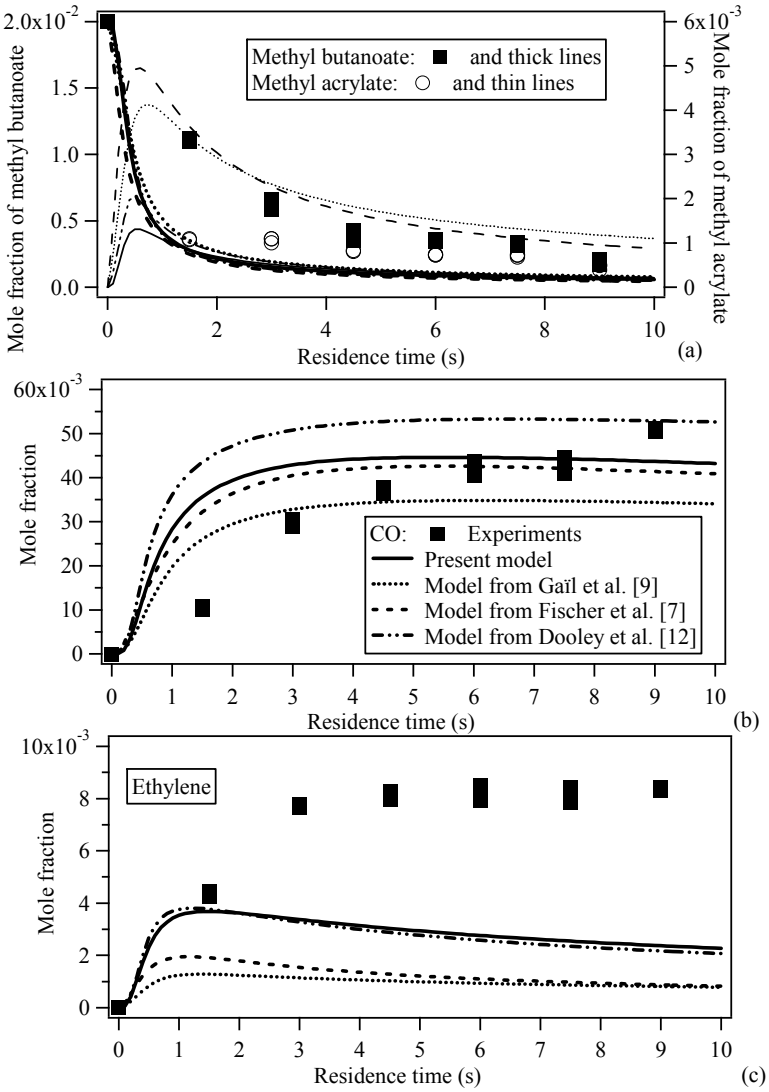

Figure 11. Comparison between the experimental results obtained in a jet-stirred reactor under the conditions of Figure 5 at 850 K and values computed using the model described in this paper and the mechanisms of Fischer et al. (7) (broken lines), Gaïl et al. (9) (dotted lines), and Dooley et al. (12) (mixed lines).

- ✓ ***Autoignition of Ethyl Butanoate***

Figure 3 shows that the agreement between experimental and simulated ignition delay times of ethyl butanoate is correct, apart from the least diluted mixtures in the upper part of the temperature range studied.

While the agreement is slightly worse for ethyl butanoate than for methyl butanoate, Figure 4 shows that the increasing difference of reactivity between both esters when temperature increases, which is experimentally observed, is modeled. However, the simulated difference of reactivity is less marked than the experimental behavior.

Discussion

Autoignition in a Shock Tube

Figure 12 displays a reaction flux analysis performed for both esters under the conditions of Figure 2, at 1370 K, the lowest temperature studied, for an equivalence ratio of 1 and for 50% conversion of ester. Figure 13 displays a sensitivity analysis showing the relative change in ignition delay times obtained when multiplying by 10 the rate constant of the main reactions consuming methyl butanoate, ethyl butanoate, and butanoic acid (a negative value means that the ignition delay time calculated with the change in rate constant is shorter). Figure 14 presents the computed temporal evolution of the initial organic reactant, the main products and •OH radicals. Figures 13 and 14 have been obtained for both esters and under the same conditions as in Figure 12.

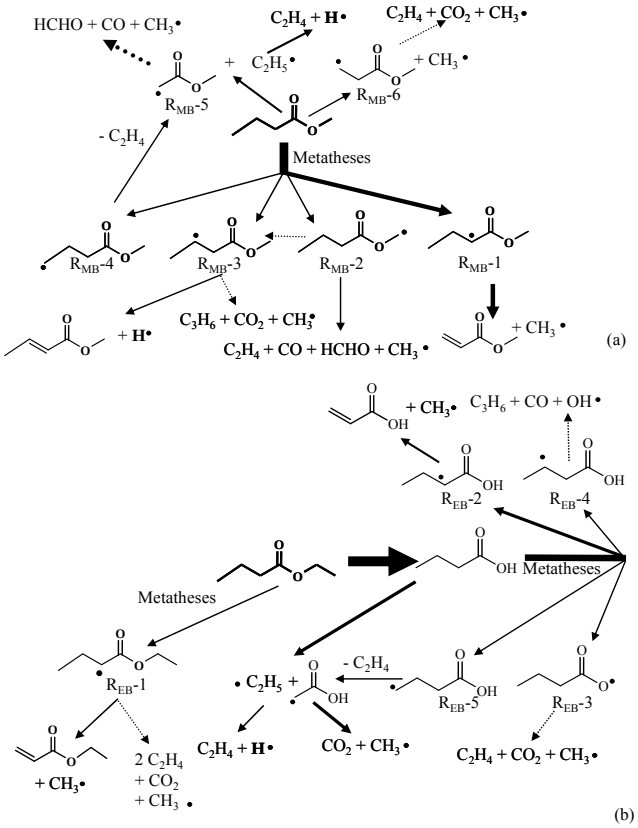

Figure 12. Reaction flux analysis performed under the conditions of Figure 2 at 1370 K for an equivalence ratio of 1 and for 50% conversion of ester in the case of (a) methyl butanoate and (b) ethyl butanoate. The size of the arrows is proportional to the relative flux. The channels involving a consumption of the esters below 5% are not shown. Dotted arrows represent several successive elementary reactions.

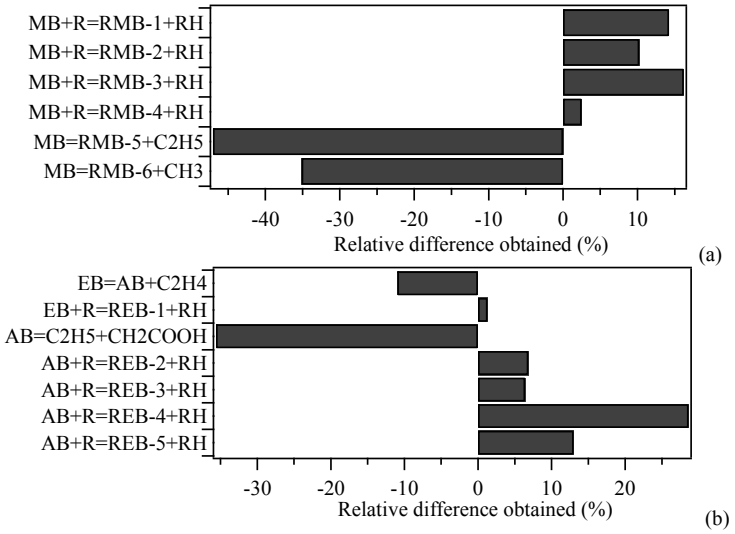

Figure 13. Sensitivity analysis showing the relative changes obtained when multiplying by 10 the rate constant of the main reactions consuming (a) methyl butanoate (MB) and (b) methyl ethanoate (EB) and butanoic acid (AB). R represents the radicals involved in H-abstractions. R_{MB}-x and R_{EB}-y refer to the radicals shown in Figure 12.

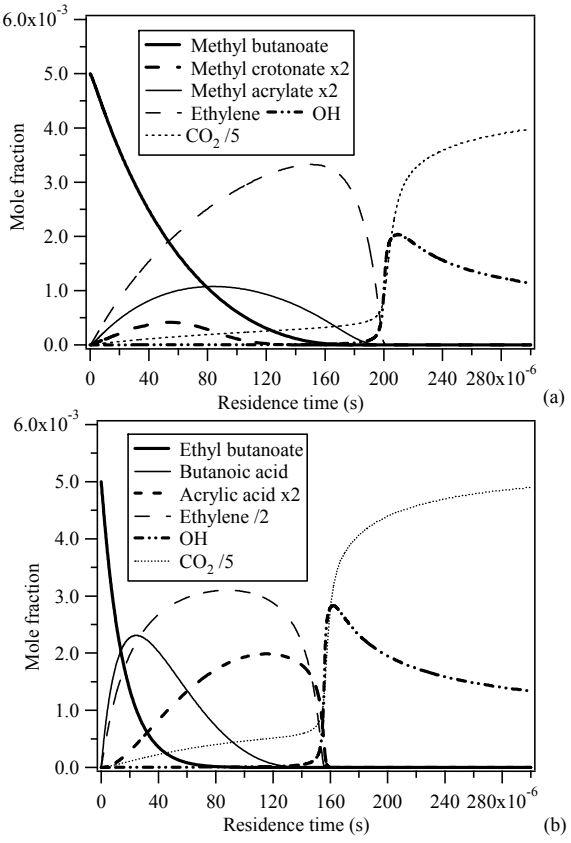

Figure 14. Temporal evolution of the initial ester, the main products, and •OH radicals under the same conditions as in Figure 12 in the case of (a) methyl butanoate and (b) ethyl butanoate.

Under the conditions of Figure 12, methyl butanoate is mainly consumed by H-abstractions by hydrogen atoms and hydroxyl radicals, which accounts for globally 75% of the ester consumption. As the abstraction of an H-atom from the atom of carbon located in α-position from the ester function has been considered as the easiest, the main radicals obtained by H-abstractions are R_{MB}-1 radicals (34% of the ester consumption) that decompose to give methyl radicals and methyl acrylate. Methyl acrylate (see Figure 14a) is the major C_{2+}-oxygenated product obtained during the autoignition of methyl butanoate. The three other isomer radicals are obtained in similar amounts. R_{MB}-2 radicals decompose to give formaldehyde and smaller radicals that ultimately lead to ethylene, carbon monoxide, and methyl radicals. Ethylene (see Figure 14a) is the major intermediate product obtained from methyl butanoate. R_{MB}-3 radicals can either produce methyl crotonate and H-atoms or propene and radicals the decomposition of which lead to carbon dioxide and methyl radicals. Methyl crotonate (see Figure 14a) is the second main C_{2+}-oxygenated product obtained during the autoignition of methyl butanoate, but it is formed in lower amounts than methyl acrylate. As shown in Figure 14a, carbon dioxide is both formed during induction time before the autoignition, and as a final product during the autoignition of methyl butanoate. R_{MB}-4 radicals yield ethylene and R_{MB}-5 radicals, which can isomerize, decompose, and ultimately lead to formaldehyde, carbon monoxide, and methyl radicals.

The second type of reactions consuming methyl butanoate is unimolecular decompositions. There are two important channels with close reaction flux and accounting for globally 25% of the ester consumption. The first one requires to break a C-C bond and leads to ethyl and R_{MB}-5 radicals (15% of the ester consumption). The decomposition of ethyl radicals leads almost only to ethylene and H-atoms. The second one involves the breaking of a C-O bond and yields methyl and R_{MB}-6 radicals, the decomposition of which is a source of carbon dioxide, ethylene and methyl radicals.

As shown in Figure 13, unimolecular decompositions of methyl butanoate to give R_{MB}-5 and ethyl radicals or R_{MB}-6 and methyl radicals have a large promoting effect as an increase of their rate constants noticeably decreases ignition delay times. This promoting effect is slightly larger in the case of the formation of R_{MB}-5 and ethyl radicals, as the decomposition of these last radicals is a source of the branching agents, H-atoms. Since the four H-abstraction channels compete with unimolecular decompositions for the ester consumption, they have a retarding effect. The important inhibiting effect of the formation of R_{MB}-3 radicals, the decomposition of which is a source of H-atoms, is certainly due to the fact that these radicals also produce unsaturated species, such as propene and methyl crotonate, which can lead by H-abstractions to resonance stabilized radicals. On the contrary, the formation of R_{MB}-2 and R_{MB}-4 radicals, which are a source of formaldehyde, which leads to •HCO radicals and then to H-atoms, has lower inhibiting effects.

The ways of consumption of ethyl butanoate are very different from those of methyl butanoate as it is mainly consumed by a molecular reaction to give butanoic acid (75% of its consumption), which is the major C_{2+}-oxygenated product obtained (see Figure 14b). As shown in Figure 14b, the formation of ethylene is twice during the oxidation of the ethyl ester (a maximum mole fraction of 6×10^{-3}) than during that of the methyl ester (a maximum mole fraction of 3.5×10^{-3}). The importance of this channel decreases when temperature increases, e.g., it accounts for only 40% of the ester consumption at $\phi = 1$ and T = 1635 K, at 50% ester conversion. It slightly increases when equivalence ratio increases, as it represents 78% of the ester consumption at $\phi = 2$ and T = 1370 K, at 50% ester

conversion. It can be observed in Figure 14b that contrary to the case of methyl butanoate, the ignition of ethyl butanoate does not occur at the end of the consumption of ester, but when butanoic acid is completely consumed.

Minor channels involve H-abstractions (22% of the ester consumption) by hydrogen atoms and hydroxyl radicals to give mainly R_{EB}-1 radicals and unimolecular decomposition (3% of the ester consumption). R_{EB}-1 radicals mainly isomerize to produce radicals that decompose to ethylene and radicals that in turn decompose to carbon dioxide and propyl radicals. These last radicals yield ethylene and methyl radicals. A small part of R_{EB}-1 radicals directly decomposes to give methyl radicals and ethyl acrylate, the second main C_{2+}-oxygenated product obtained from ethyl butanoate (see Figure 14b).

Butanoic acid is mainly consumed by H-abstractions (56% of its consumption) and yields mainly R_{EB}-2 radicals and to a lower extent R_{EB}-3, R_{EB}-4, and R_{EB}-5 radicals. R_{EB}-2 radicals are decomposed to give methyl radicals and acrylic acid, another very minor C_{2+}-oxygenated product obtained from ethyl butanoate. R_{EB}-3 radicals decompose to produce carbon dioxide and propyl radicals, a source of ethylene and methyl radicals. The decomposition of REB-4 radicals leads to propene and radicals, the decomposition of which gives carbon monoxide and hydroxyl radicals. Finally, the breaking of a C-C bond in R_{EB}-5 radicals produces ethylene and radicals, the decomposition of which yields carbon dioxide and methyl radicals. As in the case of methyl butanoate, carbon dioxide is both formed during the induction time and as a final product of the autoignition of ethyl butanoate (see Figure 14b).

Unimolecular initiations, which lead to ethyl radicals, a source of H-atoms, and radicals the decomposition of which produces methyl radical and carbon dioxide, are responsible for 32% of the consumption of butanoic acid. The unimolecular initiation yielding ethyl radicals is made easier in the acid due to a lower activation energy (78.9 kcal/mol) compared to those for the ethyl (81.2 kcal/mol) and methyl (81.7 kcal/mol) esters and also to a larger A-factor in the case of the acid. As shown in Figure 13b, this reaction has a large promoting effect, whereas the concurrent H-abstraction have an inhibiting one.

The fact that about 24% of the consumption of ethyl butanoate leads to unimolecular initiations involving the production of branching agents, H-atoms, while it is only the case for 15% from methyl butanoate certainly explains the higher reactivity observed for the ethyl ester. The fact that the importance of unimolecular initiations increases with temperature explains that the higher the temperature, the larger this difference is.

Oxidation in a Jet-Stirred Reactor

The large overestimation of the reactivity (Figure 5) and the underestimation of the formation of ethylene (Figure 7) are all the more surprising since the jet-stirred reactor has been used under conditions for which it has been proved to have a very good mixing (21) and with a temperature gradient inside the vessel below 5 K. These discrepancies could be due to possible molecular decomposition paths of the fuel, which are not taken in account in the model and which could compete with more reactive radical consumption routes. El-Nahas et al. (37) performed ab initio

calculations to investigate the possible molecular decomposition paths of methyl butanoate. To explain the formation of ethylene, which is underpredicted by our model, we tried to include these new reactions but with almost no effect on both the reactivity and the ethylene formation in our conditions. The easiest pericyclic elimination involved an activation energy of 68 kcal mol^{-1} and has no influence on our calculations. The study of the thermal decomposition of methyl butanoate would help to better understand the specific molecular decomposition chemistry of this kind of species. Dooley et al. (12) investigated the possible heterogeneous wall-catalyzed decomposition of methyl butanoate in order to reproduce the formation of methanol. The inclusion of this reaction in their model induced higher concentrations of methanol but also higher conversions of the fuel. In our case, all models predict higher conversions, which could also be explained by a wall-catalyzed paths forming unreactive species.

The overestimation of the reactivity is responsible for the displacement toward the smallest residence times and the larger magnitude of the maximum in the profiles of methyl crotonate and methyl acrylate. However, the ratio between the mole fractions of these two compounds is correctly predicted by our model.

Figure 15 displays a reaction flux analysis performed for methyl butanoate under the conditions of Figure 5, at 800 K, the lowest temperature studied, and for a residence time of 1.9 s corresponding to a 50% conversion of ester. Note that our model is too reactive compared to the experiments and some consumption routes are likely more important than they are in the reality due to this to high reactivity (e.g., low-temperature reactions).

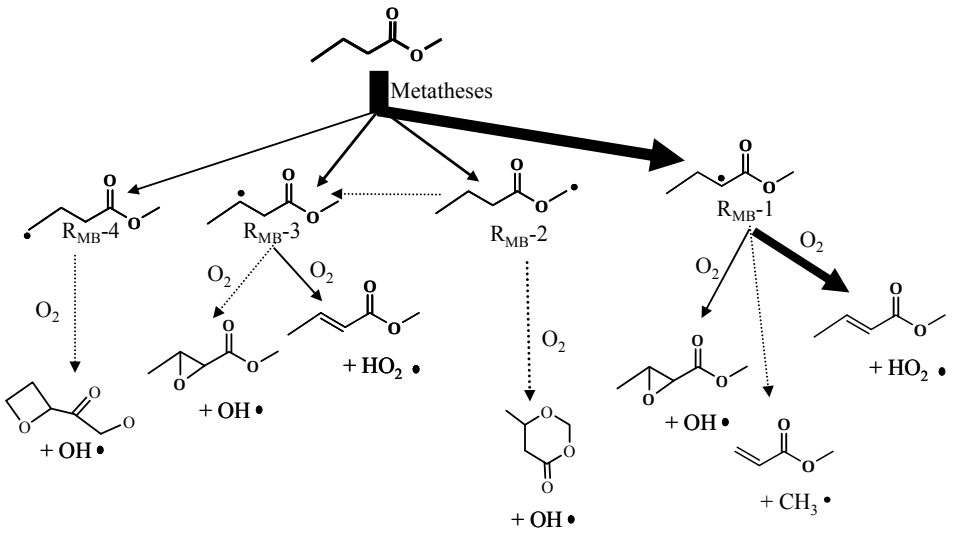

Figure 15. Reaction flux analysis performed under the conditions of Figure 5 at 800 K and for a residence time of 1.9 s corresponding to 50% conversion of methyl butanoate. The size of the arrows is proportional to the relative flux. The channels involving a consumption of the esters below 5% are not shown. Dotted arrows represent several successive elementary reactions.

Under the conditions of Figure 15, methyl butanoate is almost only consumed by H-abstractions by hydrogen atoms and hydroxyl and HO•2 radicals. As under shock tube conditions, R_{MB}-1 radicals are the main radicals produced (55% of the ester consumption). They react mainly with oxygen molecules to give methyl crotonate. Minor channels involve their decomposition to give methyl

radicals and methyl acrylate and their addition to oxygen molecules to form peroxy radicals. Subsequent isomerizations and decomposition from these peroxy radicals lead to hydroxyl radicals and a C_5 methyl ester including an oxirane. The important flux of formation of methyl crotonate by oxidation explains the more important prediction by the model compared to that of methyl acrylate.

The second most abundant radicals obtained are R_{MB}-2 radicals (17% of the ester consumption), which react mainly by addition to oxygen molecules to give after isomerization hydroxyl radicals and a C_5 methyl ester including a pyran. The formation of R_{MB}-3 radicals accounts for 16% of the ester consumption. These radicals also react mainly by addition to oxygen molecules to give after isomerization hydroxyl radicals and a C_5 methyl ester including an oxirane. A smaller channel involves their reaction with oxygen molecules to give methyl crotonate. The last radicals, R_{MB}-4 radicals, which derive from the abstraction of a primary H-atom (8% of the ester consumption), are consumed by addition to oxygen molecules followed by isomerizations and decomposition to give hydroxyl radicals and a C_5 methyl ester including an oxetane. The formation of methyl esters including a cyclic ether has not been experimentally observed in the present study, whereas such compounds with a five-membered ring have been analyzed in a recent study of the oxidation of methyl palmitate, a large ester showing reactivity in the low-temperature region, performed at similar conditions with the same experimental facility (47).

While Figure 15 shows that the reactions of additions to oxygen molecules and the derived channels (low-temperature reactions) have an important influence on the formation of products, Figure 5a shows that simulations using a mechanism in which these reactions have been removed lead to a small decrease of the reactivity at 800 K compared to the full mechanism. This influence is much lower at 850 K.

Conclusion

This paper presents new measurements concerning ignition delay times of methyl and ethyl butanoate in a shock tube behind reflected shock wave between 1130 and 1620 K and about the oxidation of methyl butanoate in a jet-stirred reactor at 800 and 850 K, as well as a detailed kinetic model allowing us to correctly reproduce these results under most studied conditions.

Shock tube experiments showed that ethyl butanoate is slightly more reactive than methyl butanoate. Reaction flux and sensitivity analyses let us think that this difference of reactivity would be due to easier unimolecular initiations involving the production of branching agents, H-atoms, in the case of the ethyl ester. The ways of consumption of both esters are very different due to the considerable importance of the molecular reaction yielding ethylene and butanoic acid in the case of ethyl butanoate. This molecular reaction makes ethyl esters a potential important source of carboxylic acid, which could contribute to the acidity of gas and aqueous phases of the atmosphere, and would most certainly exclude this type of molecules from the list of advisable fuel components.

Jet-stirred experiments have shown that the major C_{2+}-oxygenated products obtained during the oxidation of methyl butanoate are methyl crotonate and methyl acrylate. While simulations for shock tube conditions predict larger amounts of methyl acrylate compared to those of methyl crotonate, simulations for the jet-stirred reactor shows larger amounts of the C_5 unsaturated methyl ester.

Simulations of the oxidation at 800 K show also the possible formation of C_5 molecules involving three oxygen atoms in both ester and cyclic ether functions. Our model, as well as those in the literature, cannot correctly reproduce the conversion of methyl butanoate and the formation of ethylene observed in the jet-stirred reactor; this discrepancy can either be due to wall-catalyzed paths forming unreactive species or to misunderstood channels important for the chemistry of the oxidation of methyl butanoate under the studied range of temperatures. More studies in the same range of temperature but using a different type of reactor or of diagnostic should allow us to better understand this discrepancy.

Acknowledgements

This work has been supported by the "Région Lorraine" through the funding of the postdoc of M. Yahyaoui.

References

1. Agarwal, A.K. Prog. Energy Combust. Sci. 2007, 33, 233-271.
2. Graboski, M.S.; McCornick, R.L. Prog.Energy Combust. Sci. 1998, 24, 125-164.
3. Demirbas, A. Prog. Energy Combust. Sci. 2005, 31, 466-487.
4. Westbrook, C.K.; Pitz, W.J.; Curran, H.J. J. Phys. Chem. A 2006, 110, 6912-6922.
5. Pepiot-Desjardin P.; Pitsch, H.; Malhotra, R.; Kirby, S.R.; Boehman, A.L. Combust. Flame 2008, 154, 191-205.
6. Bünger, J.; Krahl, J.; Baum, K.; Schröder, O.; Müller, M.; Westphal, G.; Ruhnau, P.; Schulz, T.G.; Hallier, E. Arch. Toxicol. 2000, 74, 490-498.
7. Fisher, E.M.; Pitz, W.J.; Curran, H.J.; Westbrook, C.K. Proc. Combust. Inst. 2000, 28, 1579-1586.
8. Parsons, B.I; Danby, C.J. J. Chem. Soc. 1956, 1795-1798.
9. Gaïl, S.; Thomson, M.J.; Sarathy, S.M.; Syed, S.A.; Dagaut, P.; Diévart, P.; Marchese, A.J.; Dryer, F.L. Proc. Combust. Inst. 2007, 31, 305-311.
10. Metcalfe, W.K.; Dooley, S.; Curran, H.J.; Simmie, J.M.; El-Nahas, A.M.; Navarro, M.V. J. Phys. Chem. A 2007, 111, 4001-4014.
11. Metcalfe, W.K.; Togbé, C.; Dagaut, P.; Curran, H.J.; Simmie, J.M. Combust. Flame 2009, 156, 250-260.
12. Dooley, S.; Curran, H.J.; Simmie, J.M. Combust. Flame 2008, 153, 2-32.
13. Walton, S.M.; Woolridge, M.S.; Westbrook, C.K. Proc. Combust. Inst. 2009, 32, 255-262.
14. Huynh, L.K; Violi, A. J. Org. Chem. 2008, 73(1) 94-101.
15. Faroq, A.; Davidson, D.F.; Hanson, R.K.; Huynh, L.K; Violi, A. Proc. Combust. Inst. 2009, 32, 247-253.
16. Hayes, C.J.; Burgess Jr., D.R. Proc. Combust. Inst. 2009, 32, 263-270.
17. Fournet, R.; Baugé, J.C; Battin-Leclerc, F. Int. J. Chem. Kin. 1999, 31, 361-379.
18. Belmekki, N.; Glaude, P.A.; Da Costa, I.; Fournet, R.; Battin-Leclerc, F. Int. J. Chem. Kin. 2002, 34, 172-183.
19. Touchard, S.; Buda, F.; Dayma, G.; Glaude, P.A.; Fournet, R.; Battin-Leclerc, F. Int. J. Chem. Kin. 2005, 37, 451-463.
20. Yahyaoui, M.; Hakka, M.H.; Glaude, P.A; Battin-Leclerc, F. Int. J. Chem. Kin. 2008, 40, 25-33
21. Matras, D.; Villermaux, J. Chem. Eng. Sci. 1973, 28, 129137.
22. Bounaceur, R.; Da Costa, I.; Fournet, R.; Billaud, F.; Battin-Leclerc, F. Int. J. Chem. Kin. 2005, 37, 25-49.
23. Biet, J.; Hakka, M.H.; Warth, V.; Glaude, P.A.; Battin-Leclerc, F. Energy and Fuel, 2008, 22, 2258-2269.
24. Lifshitz, A.; Scheller, K.; Burcat, A.; Skinner, G.B. Combust. Flame, 1971,16 (3) 311-321.
25. Yahyaoui, M.; Djebaïli-Chaumeix, N.; Paillard, C.-E.; Touchard, S.; Fournet, R.; Glaude, P.A.; Battin-Leclerc, F., Proc. Combust. Inst. 2005, 30, 1137-1145.

26. Warth, V.; Stef, N.; Glaude, P.A.; Battin-Leclerc, F.; Scacchi, G.; Côme, G.M. Combust. Flame 1998, 114, 81-102.
27. Glaude, P.A.; Battin-Leclerc, F.; Judenherc, B.; Warth, V.; Fournet, R.; Côme, G.M.; Scacchi, G. Combust. Flame 2000, 121, 345-355.
28. Glaude, P.A.; Warth, V.; Fournet, R.; Battin-leclerc, F.; Côme, G.M.; Scacchi, G.; Dagaut, P.; Cathonnet, M. Energ. Fuels, 2002, 16, 1186-1195.
29. Buda, F.; Bounaceur, R.; Warth, V.; Glaude, P.A.; Fournet, R.; Battin-Leclerc, F. Combust. Flame, 2005, 142, 170-186.
30. Barbé, P.; Battin-Leclerc, F.; Côme, G.M. J Chim Phys 1995, 92,1666-1692.
31. Troe, J. Ber Buns Phys Chem 1974, 78, 478-485.
32. Muller, C.; Michel, V.; Scacchi G.; Côme, G.M. J Chim Phys 1995, 92, 1154.
33. Benson, S.W. Thermochemical kinetics, 2nd ed.; John Wiley, New York, 1976.
34. Kee, R.J.; Rupley, F.M.; Miller, J.A. Sandia Laboratories Report, SAND 89-8009B, 1993.
35. Luo, Y.R. Handbook of bond dissociation energies in organic compounds, CRC Press; Boca Raton, 2003.
36. HadjAli, K.; Crochet, M.; Vanhove, G.; Ribaucour, M. ; Minetti, R. Proc. Combust. Inst. 2009, 32, 239-246.
37. El-Nahas, A.; Navarro, M.V.; Simmie, J.M.; Bozzelli, J.W.; Curran, H.J.; Dooley, S.; Metcalfe, W. J. Phys. Chem. A 2007, 111, 3727-3739.
38. Dean, A. M.; Bozzelli J. W. Combustion Chemistry of Nitrogen, in Gas-phase Combustion Chemistry, Gardiner W.C. Ed., Springer-Verlag, New York, 2000.
39. Glaude, P.A.; Battin-Leclerc, F.; Fournet R.; Warth, V.; Côme, G.M.; Scacchi, G. Combust. Flame, 2000, 122, 451-62.
40. Frisch, M. J. et al. Gaussian03, revision B05; Gaussian, Inc., Wallingford, CT, 2004.
41. Baulch, D.L.; Cobos, C.J.; Cox, R.A.; Frank, P.; Hayman, G.D.; Just, T.; Kerr, J.A.; Murrells, T.P.; Pilling, M.J.; Troe, J.; Walker, R.W.; Warnatz, J. Combust. Flame 1994, 98, 59-79.
42. Blades, A.T. Can. J. Chem. 1954, 32, 366-372.
43. Swihart, M.T.; Carr, R.W. Int. J. Chem. Kinet. 1996, 28, 817-828.
44. Barnard, J.A.; Cocks, A.T.; Parrott, T.K. J. Chem. Soc. Faraday Trans. 1 1976, 72, 1456-1463.
45. Kairaitis, D.A.; Stimson, V.R. Aust. J. Chem. 1968, 21, 1349-1354.
46. Hall, J. M.; Rickard, M.J.A.; Petersen, E. L. Combust. Sci. Techol. 2005, 177, 455-483.
47. Hakka, M. H.; Glaude, P. A.; Herbinet, O.; Battin-Leclerc F. Combust Flame 2009, 156, 2129–2144.